Research Papers

# Structure analysis of the ribosomal intergenic spacer region of *Phaeoacremonium italicum* as a study model

Meriem LAIDANI[1,2], Maria Luisa RAIMONDO[1,*], Anna Maria D'ONGHIA[2], Antonia CARLUCCI[1,*]

[1] *Department of Agriculture, Food, Natural resources and Engineering (DAFNE), University of Foggia, 71122 Foggia, Italy*
[2] *Mediterranean Agronomic Institute of Bari, 70010 Valenzano (BA), Italy*
*Corresponding authors. E-mail: marialuisa.raimondo@unifg.it; antonia.carlucci@unifg.it

**Summary.** Increasing recognition of novel *Phaeoacremonium* species, and their recent taxonomic reassignment through phylogeny based on the β-tubulin and actin genes, have highlighted the presence of paraphyly, intraspecific variation, and incongruence of some *Phaeoacremonium* species. This study investigated the intergenic spacer rDNA regions of a representative collection of 31 *Phaeoacremonium italicum* strains, and compared their structures with those of the closest related species, *Phaeoacremonium alvesii* and *Phaeoacremonium rubrigenum*. These intergenic spacer sequences had five categories of repeat elements that were organised into distinct patterns. Morphological analyses of the *P. italicum* strains provided a more detailed description of *P. italicum*. The phylogenetic tree constructed using the intergenic spacer sequences compared with that obtained by combined analysis of β-tubulin and actin sequences indicated that the intergenic spacer rDNA region distinguished intraspecific and interspecific variations. Further molecular studies are required to determine whether intergenic spacer sequences can improve precision in defining *Phaeoacremonium* phylogeny, and prevent misidentification and the introduction of vague species boundaries for the genus.

**Keywords.** IGS, intraspecific variation, interspecific variation, *Phaeoacremonium* species.

## INTRODUCTION

The genus *Phaeoacremonium* (*Togniniales, Togniniaceae*) was originally described in 1996, containing only six species (Crous *et al.,* 1996). Ten years later, Mostert *et al.* (2006) described *Togninia* as the sexual morph of *Phaeoacremonium*, and defined 22 *Phaeoacremonium* and ten *Togninia* species. Gramaje *et al.* (2015) included *Togninia* in *Phaeoacremonium* genus, according to the change to single nomenclature for fungi (Hawksworth *et al.,* 2011). The number of described *Phaeoacremonium* species has continued to

increase to the present 63 (Ariyawansa *et al.,* 2015; Crous *et al.,* 2016; Da Silva *et al.,* 2017; Spies *et al.,* 2018), which also includes the report of *P. thailandense* from freshwater in Thailand (Calabon *et al.,* 2021).

*Phaeoacremonium* has a wide host range and worldwide distribution. The host range includes woody plants, insect larvae, freshwater and humans, and species have been reported from South, Central and North America, Asia, Europe, the Middle East, the Far East, Oceania and Africa (Gramaje *et al.,* 2015; Spies *et al.,* 2018). Many reports have associated *Phaeoacremonium* species with vascular wood diseases of several plants (Damm *et al.,* 2008; Nigro *et al.,* 2013; Raimondo *et al.,* 2014; Carlucci *et al.,* 2015; Olmo *et al.,* 2015; Spies *et al.,* 2018), where the grapevine trunk diseases, such as Esca and Petri diseases, are considered to be the most destructive and severe. To date, 36 *Phaeoacremonium* species have been isolated abundantly from necrotic wood of grapevines showing Esca and Petri diseases in vineyards, of which 22 species were in Europe and Mediterranean countries (Essakhi *et al.,* 2008; Raimondo *et al.,* 2014; Gramaje *et al.,* 2015; Jayawardena *et al.,* 2018; Spies *et al.,* 2018). *Phaeoacremonium* species have also been isolated from different woody hosts, including olive and other fruit trees that show wilt, decline, dieback and cankers. In particular, 13 *Phaeoacremonium* species have been associated with olive trees, and 34 with fruit trees, of which ten were on olive and 18 were on fruit trees in Europe and Mediterranean countries (Crous and Gams, 2000; Mostert *et al.,* 2006; Nigro *et al.,* 2013; Carlucci *et al.,* 2015; Gramaje *et al.,* 2015; Soltaninejad *et al.,* 2017; Spies *et al.,* 2018; Sohrabi *et al.,* 2020).

The recent taxonomic reassignment and the increasing recognition of novel *Phaeoacremonium* species associated with various woody host plants has highlighted the intraspecific genetic variation and paraphyly within several species-level clades, and also incongruence or lack of resolution for some *Phaeoacremonium* species using β-tubulin and actin sequences (Gramaje *et al.,* 2015; Spies *et al.,* 2018). For example, in the *Phaeoacremonium italicum/ Phaeoacremonium alvesii* group, the phylogenetic position of some strains (e.g., CBS 113590) was incongruent among the combined and individual phylogenies. Spies *et al.* (2018) also reported that the morphological differences described for these closely related species did not correspond to the intraspecific genetic variation observed, and for this reason, morphology cannot be useful to clarify species identity of strains that have unresolved phylogenetic identities.

To improve the resolution of some *Phaeoacremonium* clades, further phylogenetic markers need to be investigated. To date, few studies have attempted to use other genes as putative markers for molecular identification of *Phaeoacremonium* species. Mostert *et al.* (2005) sequenced the calmodulin gene of 19 *Phaeoacremonium* strains that belonged to 11 species to provide greater clarity on the status of the taxa closely related to *Phaeoacremonium rubrigenum*, although the calmodulin gene did not distinguish between *P. alvesii* and *P. rubrigenum* (the closest species), as the sequences were identical. Together with the internal transcribed spacer (ITS) and the β-tubulin and actin genes, Úrbez-Torres *et al.* (2014) sequenced elongation factor (EF)1-α from 56 strains that belonged to 31 *Phaeoacremonium* species, and performed multilocus analyses. The tree obtained by inclusion of the EF1-α DNA marker improved the molecular characterisation and increased the phylogenetic resolution within *Phaeoacremonium*.

Several studies have reported that the nuclear ribosomal DNA (rDNA) intergenic spacer (rDNA IGS) region could be suitable to define evolutionary dynamics of divergent species and populations, to detect genetic variability, and to develop diagnostic markers and carry out phylogenetic analyses (Sugita *et al.,* 2002; Dissanayake *et al.,* 2009; Sampietro *et al.,* 2010; Mirete *et al.,* 2013). The IGS rDNA region has been used to confirm interspecific differentiation and intraspecific discrimination among vegetative compatibility groups of *Verticillium dahliae* (Papaioannou *et al.,* 2013), and to investigate relationships in other fungi at interspecific and intraspecific levels, including for *Metarhizium anisopliae* (Pipe *et al.,* 1995), *Microdochium nivale* (Mahuku *et al.,* 1998), *Hebeloma cylindrosporium* (Guidot *et al.,* 1999), *Cryptococcus neoformans* (Diaz *et al.,* 2005) and *Phomopsis helianthi* (Pecchia *et al.,* 2004).

The present study aimed to investigate the structure of the IGS rDNA regions of a representative collection of *P. italicum* strains as a study model, and to compare them with strains of the closely related species *P. alvesii* and *P. rubrigenum*, to emphasise intraspecific and interspecific genetic variations. For these purposes, the entire IGS regions of 31 *P. italicum*, two *P. alvesii* and two *P. rubrigenum* strains were amplified and sequenced to define the IGS structures. To determine whether morphological features corresponded with putative intraspecific and interspecific genetic variation expressed by the IGS rDNA region, a detailed microscopy study of *P. italicum* strains was also carried out. To verify that IGS rDNA could be used to discriminate the *Phaeoacremonium* species, it was also amplified and sequenced in another 12 *Phaeoacremonium* species. These data were used to obtain a phylogenetic tree and to compare this with that obtained by the markers presently used for molecular identification of *Phaeoacremonium* species.

## MATERIALS AND METHODS

### Fungal isolates

This study included a total of 57 isolates of *Phaeoacremonium* that were obtained from different hosts and localities, with 49 isolates from the collection of the Department of Agriculture, Food, Natural resources and Engineering (DAFNE), University of Foggia (Italy), one isolate from Instituto de Ciencias de la Vid y del Vino (ICVV) (Spain), and seven isolates from Westerdijk Fungal Biodiversity Institute (CBS, Utrecht, The Netherlands). Two isolates of *Pleurostoma richardsiae* from DAFNE were included in this study as outgroups (Table 1).

### DNA extraction, PCR and sequencing

Genomic DNA was extracted from fresh mycelia for each isolate, using the methods of Carlucci *et al.* (2013). Partial sequences of the β-tubulin and actin genes of each of the strains were amplified according to the protocols and conditions described by Raimondo *et al.* (2014). The IGS rDNA region flanking 28S and 18S of each of the strains was amplified using the universal primers LR12R (5'-GAACGCCTCTAAGTCAGAATCC-3'; anchored in the 3' of the LSU gene) and invSR1R (5'-ACTGGCAGAATCAACCAGGTA -3'; anchored in the 5' of SSU of the RNA gene) (Durkin *et al.,* 2015).

The PCR reactions were each performed in a thermal cycler (C-1000 Touch; BioRad) in a final volume of 25 μL. The reaction mixture contained 1× PCR buffer, 3 mM MgCl$_2$, 200 μM deoxynucleotide triphosphates, 0.2 μM of each primer, 1.25 U *Taq* polymerase, and 30 ng template DNA. The *Taq* polymerase (LA Taq long-PCR), nucleotides, MgCl$_2$ and buffer were supplied by TaKaRa Bio Europe. The PCR protocol and conditions were optimised for *P. italicum*, which included 95°C denaturation for 10 min, followed by 25 cycles of denaturation at 95°C for 1 min, annealing at 55°C for 1 min, and extension at 72°C for 2.5 min; with a final extension step at 72°C for 10 min. The same PCR conditions were used for all of the *Phaeoacremonium* species, except for *P. parasiticum* and *P. croatiense*, for which the annealing temperatures were 58°C for *P. parasiticum* and 62°C for *P. croatiense.* For amplifications of the two *P. richardsiae* strains were used PCR conditions of 30 cycles, with annealing temperature of 58°C.

The sequencing was performed in both directions for all of the fungal isolates by Eurofins Genomics. As the complete fragments of the IGS regions were large, the design of additional internal primers was needed (Table 2). The sequence of each locus was assembled and manually corrected (BioEdit version 7.0.9; http://www.mbio.ncsu.edu/BioEdit). The taxonomic identification of the Italian *Phaeoacremonium* strains through BLAST searches was carried out considering threshold similarity values of 98 to 100%, and as comparisons of the β-tubulin and actin sequences with the reference strains as the ex-types. All of the novel DNA sequences generated in this study were deposited to GenBank (Table 1).

### Structure analysis of the intergenic spacer region of P. italicum

The IGS sequences obtained from each of the strains were aligned using the online multiple alignment programme MAFFT v.7 (http://mafft.cbrc.jp/alignment/server/) (Katoh and Frith, 2012; Katoh and Standley, 2013), with the iterative refinement method E-INS-I, as recommended for <200 sequences with multiple conserved domains and long gaps. The alignment was checked visually and adjusted manually where necessary. As the sequences were very large, to determine the distribution of polymorphisms among the *P. italicum* strains and those that belonged to the closest species (i.e., *P. alvesii*, *P. rubrigenum*), the GeneQuest program of the Lasergene 6 software package was used (DNAstar). The pairwise identities of the IGS sequences were evaluated using MegAlign version 15 (DNAstar, Madison, WI, USA).

### Morphology

The growth rates of the *P. italicum* isolates were determined over 8 d and 16 d on malt extract agar (MEA; 50 g malt extract agar (Oxoid), 1 L water), potato dextrose agar (PDA; 39 g potato dextrose agar (Oxoid), 1 L water), and oatmeal agar (OA; 30 g oats, 8 g agar (Oxoid), 1 L water), with incubations at 23±2°C. The cardinal temperatures for growth of each isolate were determined on MEA, with incubations in the dark at temperatures from 5°C to 40°C, at 5°C intervals, and including 37°C. Colony morphologies were determined on MEA, PDA and OA after 21 d at 23±2°C, and colony colours were determined using the colour charts of Rayner (1970).

Micromorphological characterisation of each isolate was performed according to Raimondo *et al.* (2014). The dimensions and morphologies of the conidiophore structures, and the sizes, phialide types and shapes, presence of bundles, and conidium shapes and sizes were measured from 100% lactic acid mounts as 30 measurements (×100 magnification), using a measurement module

**Table 1.** Hosts, origins and sources of *Phaeoacremonium* spp. isolates used in this study.

| Species | Isolate code | Host | Origin | Source | Sub-group | GenBank β-tubulin | GenBank Actin | GenBank IGS |
|---|---|---|---|---|---|---|---|---|
| *P. alvesii* | CBS 113590 | *Dodonaea viscosa* | Australia | CBS | #7 | AY579304 | AY579237 | MZ468465 |
| | CBS 408.78 | *Homo sapiens* | USA | CBS | - | AY579303 | AY579236 | MZ468464 |
| | CBS 729.97 | *Homo sapiens* | USA | CBS | - | AY579302 | AY579235 | MZ468463 |
| *P. amygdalinum* | Pm10 | *Prunus dulcis* | Foggia (FG), Apulia, Italy | DAFNE | - | MW714562 | MW716265 | MZ468466 |
| *P. croatiense* | Pm120 | *Vitis vinifera* | Campomarino (CB), Molise, Italy | DAFNE | - | MZ442499 | MZ442548 | MZ468467 |
| *P. fraxinopennsylvanicum* | Pm182 | *Vitis vinifera* | Torremaggiore (FG), Apulia, Italy | DAFNE | - | MZ442501 | MZ442542 | MZ468468 |
| *P. griseorubrum* | CBS 111657$^T$ | *Homo sapiens* | Maryland, Texas, USA | CBS | - | AY579294 | AY579227 | MZ468516 |
| *P. hispanicum* | CBS 123910 | *Vitis vinifera* | Valencia, Spain | ICVV | - | FJ517164 | FJ517156 | MZ468519 |
| *P. iranianum* | Pm121 | *Vitis vinifera* | Campomarino (CB), Italy | DAFNE | - | MZ442494 | MZ442543 | MZ468469 |
| | Pm122 | *Vitis vinifera* | Campomarino (CB), Italy | DAFNE | - | MZ442495 | MZ442544 | MZ468470 |
| *P. italicum* | Pm1 | *Olea europaea* | Canosa di Puglia (BT), Apulia, Italy | DAFNE | #1 | KJ534074 | KJ534046 | MZ468517 |
| | Pm2 | *Olea europaea* | Canosa di Puglia (BT), Apulia, Italy | DAFNE | #1 | MZ442459 | MZ442506 | MZ468471 |
| | CBS 137763$^T$ Pm19 | *Vitis vinifera* | San Severo (FG), Apulia, Italy | DAFNE | #1 | MZ442458 | MZ442507 | MZ468472 |
| | CBS 137764 Pm20 | *Vitis vinifera* | Cerignola (FG), Apulia, Italy | DAFNE | #1 | KJ534075 | KJ534047 | MZ468518 |
| | Pm32 | *Vitis vinifera* | Torremaggiore (FG), Apulia, Italy | DAFNE | #1 | KJ534080 | KJ534052 | MZ468473 |
| | Pm33 | *Vitis vinifera* | Cerignola (FG), Apulia, Italy | DAFNE | #1 | KJ534081 | KJ534053 | MZ468474 |
| | Pm38 | *Olea europaea* | Canosa di Puglia (BT), Apulia, Italy | DAFNE | #1 | MZ442460 | MZ442508 | MZ468475 |
| | Pm54 | *Olea europaea* | Cerignola (FG), Apulia, Italy | DAFNE | #1 | MZ442461 | MZ442509 | MZ468476 |
| | Pm103 | *Olea europaea* | San Giovanni Rotondo, (FG), Apulia, Italy | DAFNE | #1 | MZ442462 | MZ442510 | MZ468477 |
| | Pm35M | *Olea europaea* | San Giovanni Rotondo, (FG), Apulia, Italy | DAFNE | #2 | MZ442463 | MZ442511 | MZ468478 |
| | Pm31M | *Prunus dulcis* | San Giovanni Rotondo, (FG), Apulia, Italy | DAFNE | #2 | MZ442464 | MZ442512 | MZ468479 |
| | Pm290M | *Prunus dulcis* | San Giovanni Rotondo, (FG), Apulia, Italy | DAFNE | #2 | MZ442465 | MZ442513 | MZ468480 |
| | Pm340M | *Olea europaea* | San Giovanni Rotondo, (FG), Apulia, Italy | DAFNE | #2 | MZ442466 | MZ442514 | MZ468481 |
| | Pm50M | *Olea europaea* | San Giovanni Rotondo, (FG), Apulia, Italy | DAFNE | #3 | MZ442467 | MZ442515 | MZ468482 |
| | Pm58 | *Vitis vinifera* | San Severo (FG), Apulia, Italy | DAFNE | #3 | MZ442468 | MZ442516 | MZ468483 |
| | Pm259 | *Olea europaea* | Mattinata (FG), Apulia, Italy | DAFNE | #3 | MZ442469 | MZ442517 | MZ468484 |
| | Pm503 | *Prunus dulcis* | Foggia (FG), Apulia, Italy | DAFNE | #3 | MZ442470 | MZ442518 | MZ468485 |
| | Pm45 | *Olea europaea* | Carpino (FG), Apulia, Italy | DAFNE | #4 | MZ442474 | MZ442519 | MZ468486 |
| | Pm60 | *Olea europaea* | Canosa di Puglia (BT), Apulia, Italy | DAFNE | #4 | MZ442475 | MZ442520 | MZ468487 |
| | Pm105 | *Prunus dulcis* | Cerignola (FG), Apulia, Italy | DAFNE | #4 | MZ442476 | MZ442521 | MZ468488 |
| | Pm199 | *Vitis vinifera* | Torremaggiore (FG), Apulia, Italy | DAFNE | #4 | MZ442477 | MZ442522 | MZ468489 |
| | Pm303 | *Vitis vinifera* | Cerignola (FG), Apulia, Italy | DAFNE | #4 | MZ442478 | MZ442523 | MZ468490 |
| | Pm17 | *Olea europaea* | Monte Sant'Angelo (FG), Apulia, Italy | DAFNE | #5 | MZ442479 | MZ442524 | MZ468491 |
| | Pm15 | *Olea europaea* | Monte Sant'Angelo (FG), Apulia, Italy | DAFNE | #5 | MZ442480 | MZ442525 | MZ468492 |
| | Pm22 | *Olea europaea* | Monte Sant'Angelo (FG), Apulia, Italy | DAFNE | #5 | MZ442481 | MZ442526 | MZ468493 |

(Continued)

**Table 1.** (Continued).

| Species | Isolate code | Host | Origin | Source | Sub-group | GenBank | | |
|---|---|---|---|---|---|---|---|---|
| | | | | | | β-tubulin | Actin | IGS |
| | Pm180 | *Vitis vinifera* | Torremaggiore (FG), Apulia, Italy | DAFNE | #5 | MZ442482 | MZ442527 | MZ468494 |
| | Pm196 | *Vitis vinifera* | Stornarella (FG), Apulia, Italy | DAFNE | #5 | MZ442483 | MZ442528 | MZ468495 |
| | Pm210 | *Vitis vinifera* | Cerignola (FG), Apulia, Italy | DAFNE | #5 | MZ442484 | MZ442529 | MZ468496 |
| | Pm235 | *Olea europaea* | Cerignola (FG), Apulia, Italy | DAFNE | #5 | MZ442485 | MZ442530 | MZ468497 |
| | Pm250 | *Prunus dulcis* | Foggia (FG), Apulia, Italy | DAFNE | #5 | MZ442486 | MZ442531 | MZ468498 |
| | Pm59 | *Olea europaea* | Canosa di Puglia (BT), Apulia, Italy | DAFNE | #6 | MZ442487 | MZ442532 | MZ468499 |
| | Pm61 | *Olea europaea* | Canosa di Puglia (BT), Apulia, Italy | DAFNE | #6 | MZ442488 | MZ442533 | MZ468500 |
| | Pm231 | *Vitis vinifera* | Stornara (FG), Apulia, Italy | DAFNE | #6 | MZ442489 | MZ442534 | MZ468501 |
| | Pm297 | *Vitis vinifera* | Canosa di Puglia (BT), Apulia, Italy | DAFNE | #6 | MZ442490 | MZ442535 | MZ468502 |
| *P. minimum* | Pm35 | *Olea europaea* | Carpino (FG), Apulia, Italy | DAFNE | - | MZ442473 | MZ442538 | MZ468503 |
| | Pm39 | *Olea europaea* | Torremaggiore (FG), Apulia, Italy | DAFNE | - | MZ442472 | MZ442537 | MZ468504 |
| | Pm41 | *Olea europaea* | Vieste (FG), Apulia, Italy | DAFNE | - | MZ442471 | MZ442536 | MZ468505 |
| *P. oleae* | Pm14 | *Olea europaea* | Carpino (FG), Apulia, Italy | DAFNE | - | MW714563 | MW714561 | MZ468506 |
| | Pm46 | *Olea europaea* | Carpino (FG), Apulia, Italy | DAFNE | - | MZ442500 | MZ442546 | MZ468507 |
| *P. parasiticum* | Pm88 | *Olea europaea* | Stornara (FG), Apulia, Italy | DAFNE | - | KM201220 | KM201190 | MZ468508 |
| | Pm388 | *Vitis vinifera* | Torremaggiore (FG), Apulia, Italy | DAFNE | - | MZ442498 | MZ442547 | MZ468509 |
| *P. rubrigenum* | CBS 498.94 ᵀ | *Homo sapiens* | USA | CBS | - | MZ442502 | AY579238 | MZ468510 |
| | CBS 112046 | *Homo sapiens* | USA | CBS | - | MZ442503 | AY579239 | MZ468511 |
| *P. scolyti* | CBS 113597ᵀ | *Vitis vinifera* | Wellington, Western Cape Province, S. Africa | CBS | - | AF246800 | AY579224 | MZ468462 |
| | Pm5 | *Olea europaea* | Foggia (FG), Apulia, Italy | DAFNE | - | MZ442491 | MZ442539 | MZ468459 |
| | Pm24A | *Vitis vinifera* | Foggia (FG), Apulia, Italy | DAFNE | - | MZ442492 | MZ442541 | MZ468460 |
| | Pm 155 | *Olea europaea* | Foggia (FG), Apulia, Italy | DAFNE | - | MZ442493 | MZ442540 | MZ468461 |
| *P. sicilianum* | Pm65 | *Olea europaea* | Cerignola (FG), Apulia, Italy | DAFNE | - | KM201209 | KM201202 | MZ468512 |
| | Pm362 | *Vitis vinifera* | Cerignola (FG), Apulia, Italy | DAFNE | - | MZ442496 | MZ442549 | MZ468513 |
| *P. viticola* | Pm34 | *Olea europaea* | Torremaggiore (FG), Apulia, Italy | DAFNE | - | MZ318696 | MZ318697 | MZ468514 |
| | Pm43 | *Vitis vinifera* | Cerignola (FG), Apulia, Italy | DAFNE | - | MZ442497 | MZ442545 | MZ468515 |
| *Pleurostoma richardsiae* | Pl4 | *Olea europaea* | Canosa di Puglia (BT), Apulia, Italy | DAFNE | - | MZ442504 | MZ468457 | MZ468520 |
| | Pl29 | *Olea europaea* | Torremaggiore (FG), Apulia, Italy | DAFNE | - | MZ442505 | MZ468458 | MZ468521 |

ᵀ, ex-type culture; CBS, Centraalbureau voor Schimmelcultures, Utrecht, The Netherlands; DAFNE, Department of Agriculture, Food, Natural Resources and Engineering, University of Foggia, Italy; ICVV, Instituto de Ciencias de la Vid y del Vino, Logroño, Spain. Bold text, strains analysed as representative of the sub-groups defined.

**Table 2.** Internal sequencing primers designed to obtain the complete sequences of the intergenic spacer rDNAs.

| Primer name | Sequence (5'->3') | Direction |
|---|---|---|
| Amygd_INT_F | 5'-GCAACCTGCTCTCGACT-3' | Forward |
| Amygd_INT_R | 5'-GACCCTAAGGTGCCACCTAT-3' | Reverse |
| Croa_INT_F | 5'-GTAGCTGCTCTCGACTTT-3' | Forward |
| Fraxy_INT_F | 5'-GCAACCTGCTCTCGACTT-3' | Forward |
| Gris_INT_R | 5'-GCCTTCCTTAGGTAGGCT-3' | Forward |
| Hispan_INT_F | 5'-GCTCTCGACCTTCTTCCA-3' | Forward |
| Hispan_INT_R | 5'-GCTAGACCTACGCACTGA-3' | Reverse |
| Iran_INT_F | 5'-GCAACCTGCTCTCGACTT-3' | Forward |
| Iran_INT_R | 5'-GCACCTTAGGGTCTAACG-3' | Reverse |
| Ital_INT_R[a] | 5'-ATATAATGTCGCAGGGTC-3' | Reverse |
| Minim_INT_R1 | 5'-GCCTCTTAGGTATCATAC-3' | Reverse |
| Minim_INT_R2 | 5'-GGCTATATCCTTATCCTACC-3' | Reverse |
| Oleae_INT_R | 5'-GCCTCTTAGGTATCCTACCT-3' | Reverse |
| Paras_INT_F | 5'-TAGTCGGATCTATAGTTAG-3' | Forward |
| Scol_INT_F | 5'-TGATATCCTTCGCGCTGG-3" | Forward |
| Vitic_INT_R | 5'-GGTCTAGCAATCTGCCAGC-3" | Forward |
| Pleuro_INT_F | 5'-TTTCACTTACCCTACACC-3' | Forward |
| Pleuro_INT_F | 5'-CTGTGATACGATGCCGGA-3' | Forward |

[a] The same internal primer was used also for *Phaeoacremonium alvesii* and *P. rubrigenum*.

(Application Suite; Leica Microsystem GmbH). The phialide types and shapes were determined according to Mostert *et al.* (2006). Photomicrographs were recorded with a digital camera (DFC320; Leica) on a DMR microscope (Leica) fitted with Nomarski differential interference contrast optics. The 5th and 95th percentiles were calculated for all of the measurements.

*Phylogenetic analyses*

The sequences of the β-tubulin and actin genes were aligned using MAFFT v.7 (http://mafft.cbrc.jp/alignment/server/) (Katoh and Standley, 2013), with the default parameters. The alignment was checked visually and improved manually where necessary. Model Finder Plus (Kalyaanamoorthy *et al.,* 2017) implemented in the IQTREE software (Nguyen *et al.,* 2015) was used to select the best-fit DNA substitution models using Bayesian information criteria. The sequences were concatenated in one dataset to perform multilocus analyses. A partitioned model with two segments was created, each with a different model of evolution estimated previously by Model Finder Plus (Kalyaanamoorthy *et al.,* 2017). Phylogenetic analyses were carried out based on maximum likelihood and maximum parsimony. Before performing the phylogenetic analyses, the presence of

different phylogenetic hypotheses in a partitioned dataset was assessed by a partition homogeneity test (i.e., an incongruence length difference test) using PAUP version 4.0b10 (Swofford, 2003). In this test, 100 datasets were artificially created by random sampling among all of the observed sites of genotypes, and then swapping sites among the loci, to obtain a *P* value. If the *P* value was >0.01, there was no incongruence among the loci, and so combination of the data improves or does not reduce the phylogenetic accuracy (Cunningham, 1997). Maximum likelihood analysis was performed using the IQTREE software (Nguyen *et al.,* 2015), with 1000 ultrafast bootstrap replicates. The ultrafast bootstrap approximation (Minh *et al.*, 2013) assesses branch supports from 10 to 40 times faster than the RAxML rapid bootstrap, and obtains less biased support values (Minh *et al.,* 2013; Hoang *et al.*, 2018). Unlike the non-parametric bootstrap, which considers bootstrap values ≥50% as statistically significant, the ultrafast bootstrap considers ≥80% as statistically significant. The maximum parsimony analysis was performed using PAUP version 4.0b10 (Swofford, 2003), with the heuristic search option, 10,000 random taxa additions, and tree bisection and reconstruction as the branch swapping algorithm. Branches of zero length were collapsed and all of the multiple, equally parsimonious trees were saved. The gaps were treated as missing data. Bootstrap support values were calculated from 1000 heuristic search replicates and 1000 random taxon additions. The tree lengths (*TL*), consistency index (*CI*), retention index (*RI*), homoplasy index (*HI*) and rescaled consistency index (*RC*) were calculated, and the resulting trees were visualised with TreeView version 1.6.6 (Page, 1996). The final tree was selected among the suboptimal trees from each run by comparison of the likelihood and bootstrap scores.

The aligned dataset of the IGS sequences was subjected to maximum likelihood and maximum parsimony analyses, as described above. Before performing the maximum likelihood analysis, the IGS dataset was first analysed with Model Finder Plus (Kalyaanamoorthy *et al.,* 2017), as described above. Two strains of *P. richardsiae* (Pl3, Pl29) were used as outgroups in all of the phylogenetic analyses.

RESULTS

*PCR amplification and sequencing*

The β-tubulin and actin genes were amplified for all of the 61 isolates and produced the expected fragments of 700 bp and 300 bp, respectively. The BLAST search and the comparison of the β-tubulin and actin sequenc-

es with the reference strains as ex-type allowed the 49 Italian strains to be attributed to 11 *Phaeoacremonium* spp., as follows: *P. amygdalinum*, *P. croatiense*, *P. fraxinopennsylvanicum* (one strain each), *P. iranianum* (two strains), *P. italicum* (30), *P. minimum* (three), *P. oleae* (two), *P. parasiticum* (two), *P. scolyti* (three), *P. sicilianum* (two) and *P. viticola* (two strains) (Table 1). The β-tubulin and actin sequences of the remaining *Phaeoacremonium* strains (seven from CBS, one from Spain) were compared with their sequences already deposited in BLAST to confirm the taxonomic identities. Therefore, the newly generated β-tubulin and actin sequences of the above-mentioned strains were not re-submitted to GenBank, except for the β-tubulin sequences of *P. rubrigenum* strains, as those present in GenBank were incomplete (Table 1).

The consensus IGS sequences obtained from 57 different strains of *Phaeoacremonium* spp. and for two *P. richardsiae* strains showed different nucleotide lengths, which ranged from 2088 bp to 2427 bp. The IGS sequence lengths among the *P. italicum* strains were also variable, and ranged from 2264 bp to 2300 bp. Analysis of the complete IGS sequences showed that the 5S rDNA gene was not found, and thus the IGS consists of a single uninterrupted region between the end of the large subunit (LSU) region and the beginning of the next small subunit (SSU) region.

*Structural analysis of the intergenic spacer region of* Phaeoacremonium italicum

The alignment obtained from all of the 59 strains (i.e., including the outgroup taxa) consisted of 3451 characters, including gaps. Based on the differences observed among the aligned *P. italicum* sequences, seven different sub-groups were identified, and are indicated as sub-groups #1, #2, #3, #4, #5, #6 and #7, where, respectively, the representative strains used to analyse the structures of the IGS regions were defined as CBS 137763 (ex-type), Pm31M, Pm50M, Pm45, Pm17, Pm59 and CBS 113590 (Table 1). Three structural regions were defined: one central polymorphic region (PR, positions 231-2807) that is flanked by two conserved regions (CR1, positions 1-230; CR2, positions 2808-3451) (Figure 1a). CR1 is adjacent to the 28S rDNA region, and it is a conserved sequence that ranges from 99% to 100% for pairwise identities. CR2 is adjacent to the 18S rRNA region, and is also highly conserved (99.6%-100% for pairwise identities). The polymorphisms in these two conserved regions consisted of single base substitutions (i.e., transitions and/or transversions) and small (1 or 2 bp) insertions and deletions (indels).

In contrast, PR is less conserved, with pairwise identities of 84.1%, which has resulted from variable indels and point mutations. Detailed analysis of the IGS structures of the representative *P. italicum* strains of the seven sub-groups revealed the presence of five short repeat elements that are organised in five different patterns, which are here indicated as elements A, B, C, P and R (Figure 2a, b). Element A consists of a pair of perfect repeats of 12 bp; element B consists of an imperfect direct repeat of 15 bp; element C consists of a perfect consecutive repeat of 12 bp; element P consists of a single palindromic sequence of 14 bp located before the first copy of element C; and element R is the most commonly encountered and consists of an imperfect direct repeat of 15 bp (Figure 1b and c). Based on the distributions of the short repeat elements, the central PR can be subdivided into two sub-regions, as PR-a (positions 231-1643) and PR-b (positions 1644-2807) (Figure 1b and c). Sub-region PR-a shares a common structural organisation of three short repeat elements (A, B, R) in all of the isolates.

Each of the *P. italicum* strains that belong to the first six of the sub-groups (i.e., #1 to #6) show the same structural organisation of PR-a, and contain: one perfect repeat copy of element A; nine copies of imperfect repeats of element R (R1–R9); one truncated imperfect repeat indicated here as Rt1; and one imperfect repeat of element B, indicated here as B1 (Figure 1b). Instead, PR-b starts with the element P and shows characteristic differences across the IGS. The main feature of this sub-region consists of a variable number of copies of perfect consecutive repeats of element C (2–10), and of elements R (8–9). For elements R, three (R4, R5, R8) were also contained in the PR-a region, and the other three (indicated as R10, R11 and R12) were newly encountered. In addition, two truncated imperfect repeats (Rt2 and R8t) were identified. The *P. italicum* strains of sub-groups #1, #2 and #3 show eight R elements located in the same positions, while those of sub-groups #4 and #5 show nine R elements (Figure 1b). The *P. italicum* strain of sub-group #6 shows seven R elements and lacks elements R5 and R12 (Figure 1b). Two imperfect repeats of element B, indicated here as B2 and B3, were found for PR-b, and one perfect repeat copy of element A, was found for CR2 (Figure 1b). The strain CBS 113590, representative of sub-group #7, renamed as *P. italicum sensu lato* by Spies *et al.* (2018), showed some differences inside the IGS structure. In particular, for this strain, PR-a includes the same elements of PR-a of *P. italicum* (sub-groups #1 to #6), except for the absence of element R8 (position 1088), and for its modified (*) element R, here indicated as R12* (position 1130). The PR-b has a single copy of element C, and nine elements R in the same positions as sub-groups #4 and #5 (Figure 1b).

In addition, structure analysis was carried out for the closest species to *P. italicum*, as *P. alvesii* and *P. rubrigenum*. The same repeated elements seen for the *P. italicum* sub-groups were also present in *P. alvesii* and *P. rubrigenum*, although the positioning and composition of some of these elements were different (Figure 2b, c). In particular, *P. alvesii* strain CBS 408.78 shows the same IGS structure as *P. italicum sensu lato* (CBS 113590; sub-group #7) (Figure 1c).

For the *P. alvesii* strain CBS 729.97, its PR-a has one perfect repeat copy of element A, one copy of element

B1, and nine copies (R1, R2, Rt1, R3, R4, R5, R6, R7, R9) of element R. For its PR-b, there is one copy of modified element P (P*), one copy of element C, and nine copies (R10, R5*, R8, R5, R4, Rt2, R11, R12, R8) of element R, of which R5* is modified. The CR2 is the same as for *P. italicum*, except for the modified element B3 (B3*) (Figures 1c and 2b).

For the *P. rubrigenum* strain CBS 498.94 (ex-type), PR-a shows one perfect repeat copy of element A, one copy of modified element B1 (B1*), and seven copies (R1, R2*, Rt1*, R3*, R8, R12, R9) of imperfect repeats of ele-
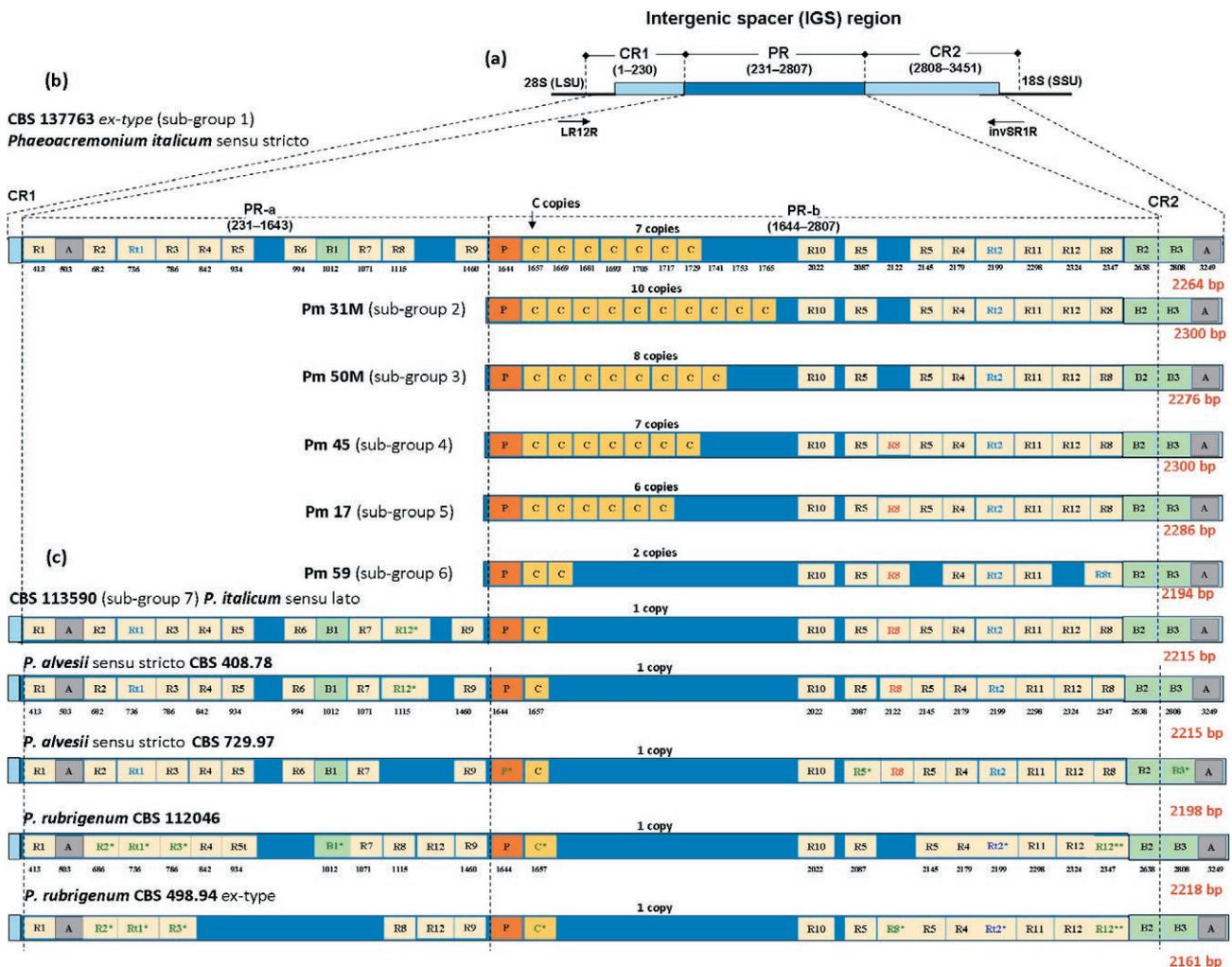


**Figure 1.** Structures of the IGS rDNA regions in *Phaeoacremonium italicum*, *P. alvesii* and *P. rubrigenum*. **(a)** Organisation of the IGS rDNA sequences into sub-regions CR1 (conserved region), PR (polymorphic region) and CR2 (conserved region), with corresponding nucleotide positions in parentheses. Arrows indicate annealing positions of PCR universal primers LR12R and invSR1R, within the extremities of the 28S and 18S rRNA genes. **(b)** Structural organisation of repeat elements A, B, C, P and R in the IGS region of *P. italicum* sub-groups #1 to #6. Numbers below indicate nucleotide bp of start positions of each element. **(c)** Structural organisation of repeat elements in the IGS region of *P. italicum* sub-group #7, *P. alvesii* and *P. rubrigenum* strains. Numbers below indicate nucleotide bp of start positions of each element. **(b** and **c)** Areas CR1 and CR2 are not shown because they have the same structural organisation in all of the isolates. Sub-region PR-b shares a structural organisation of five short repeat elements (A, B, C, P, R) in all of the isolates that are differently located on the basis of each sub-group defined.
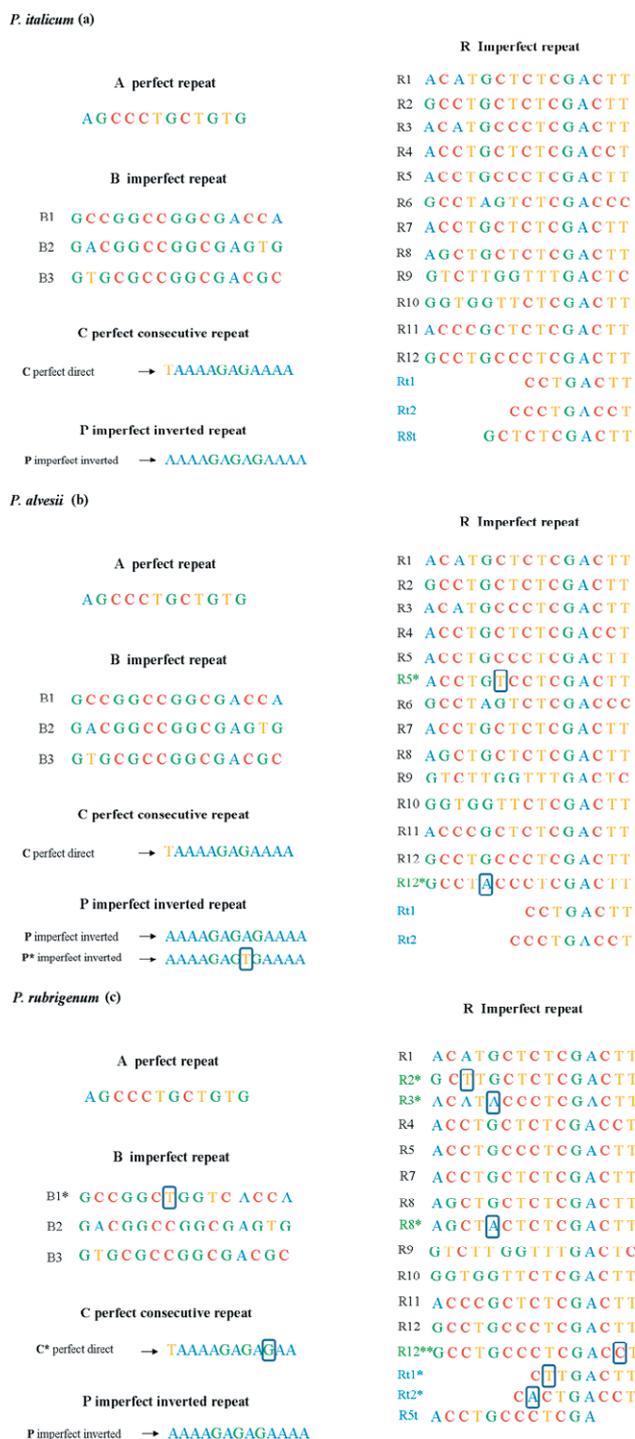
**P. italicum (a)**

**A perfect repeat**
AGCCCTGCTGTG

**B imperfect repeat**
B1 GCCGGCCGGCGACCA
B2 GACGGCCGGCGAGTG
B3 GTGCGCCGGCGACGC

**C perfect consecutive repeat**
C perfect direct → TAAAAGAGAAAA

**P imperfect inverted repeat**
P imperfect inverted → AAAAGAGAGAAAA

**R Imperfect repeat**
R1 ACATGCTCTCGACTT
R2 GCCTGCTCTCGACTT
R3 ACATGCCCTCGACTT
R4 ACCTGCTCTCGACCT
R5 ACCTGCCCTCGACTT
R6 GCCTAGTCTCGACCC
R7 ACCTGCTCTCGACTT
R8 AGCTGCTCTCGACTT
R9 GTCTTGGTTTGACTC
R10 GGTGGTTCTCGACTT
R11 ACCCGCTCTCGACTT
R12 GCCTGCCCTCGACTT
Rt1 CCTGACTT
Rt2 CCCTGACCT
R8t GCTCTCGACTT

**P. alvesii (b)**

**A perfect repeat**
AGCCCTGCTGTG

**B imperfect repeat**
B1 GCCGGCCGGCGACCA
B2 GACGGCCGGCGAGTG
B3 GTGCGCCGGCGACGC

**C perfect consecutive repeat**
C perfect direct → TAAAAGAGAAAA

**P imperfect inverted repeat**
P imperfect inverted → AAAAGAGAGAAAA
P* imperfect inverted → AAAAGA[T]GAAAA

**R Imperfect repeat**
R1 ACATGCTCTCGACTT
R2 GCCTGCTCTCGACTT
R3 ACATGCCCTCGACTT
R4 ACCTGCTCTCGACCT
R5 ACCTGCCCTCGACTT
R5* ACCTG[T]CCTCGACTT
R6 GCCTAGTCTCGACCC
R7 ACCTGCTCTCGACTT
R8 AGCTGCTCTCGACTT
R9 GTCTTGGTTTGACTC
R10 GGTGGTTCTCGACTT
R11 ACCCGCTCTCGACTT
R12 GCCTGCCCTCGACTT
R12* GCCT[A]CCCTCGACTT
Rt1 CCTGACTT
Rt2 CCCTGACCT

**P. rubrigenum (c)**

**A perfect repeat**
AGCCCTGCTGTG

**B imperfect repeat**
B1* GCCGGC[T]GGTC ACCA
B2 GACGGCCGGCGAGTG
B3 GTGCGCCGGCGACGC

**C perfect consecutive repeat**
C* perfect direct → TAAAAGAGA[G]AA

**P imperfect inverted repeat**
P imperfect inverted → AAAAGAGAGAAAA

**R Imperfect repeat**
R1 ACATGCTCTCGACTT
R2* G[C]TGCTCTCGACTT
R3* ACAT[A]CCCTCGACTT
R4 ACCTGCTCTCGACCT
R5 ACCTGCCCTCGACTT
R7 ACCTGCTCTCGACTT
R8 AGCTGCTCTCGACTT
R8* AGCT[A]CTCTCGACTT
R9 GTCTT GGTTTGACTC
R10 GGTGGTTCTCGACTT
R11 ACCCGCTCTCGACTT
R12 GCCTGCCCTCGACTT
R12** GCCTGCCCTCGAC[C]T
Rt1* C[T]TGACTT
Rt2* [G]ACTGACCT
R5t ACCTGCCCTCGA

**Figure 2.** DNA short repeat elements A, B, C, P and R and their variants observed in the *Phaeoacremonium italicum*, *P. alvesii* and *P. rubrigenum* strains. Boxes indicate all polymorphic bases in elements B and R modified (R*).

ment R, of which three (R2*, Rt1*, R3*) were modified. Its PR-b shows one copy of element P, one copy of modified element C (C*), and nine copies (R10, R5, R8*, R5, R4, Rt2*, R11, R12, R12**) of imperfect repeats of element R, of which three (R8*, Rt2*, R12**) were modified (Figures 1c and 2c). For the *P. rubrigenum* strain CBS 112046, PR-a has one perfect repeat copy of element A and ten copies (R1, R2*, Rt1*, R3*, R4, R5t, R7, R8, R12, R9) of imperfect repeats of element R, of which three (R2*, Rt1*, R3*) were modified. PR-b has one copy of modified element C (C*) and eight copies (R10, R5, R5, R4, Rt2*, R11, R12, R12**) of imperfect repeats of element R, of which two (Rt2*, R12**) were modified. For *P. rubrigenum* strain CBS 112046, CR2 is the same as for *P. italicum* (Figures 1c and 2c).

### Morphology

The morphological features of the representative isolates of each sub-group of *P. italicum* in culture are outlined in Table 3. The strains that belonged to sub-groups #1 to #6 (respectively, CBS 137763, Pm31, Pm50M, Pm45, Pm17, Pm59) have similar morphologies and culture features. The mycelia consisted of branched and septate hyphae that occurred singly or in bundles, and rarely had tuberculate hyphae, with sub-hyaline to pale brown, verruculose to smooth warts. Unbranched conidiophores were frequently observed, occasionally narrower at the bases, erect, with up to nine septate (generally three or four septate) and each ending in a single terminal phialide, which often had one or two lateral phialides of type II next to the terminal phialide. Percurrent rejuvenation was frequently observed (Figure 3).

Branched conidiophores with different levels of branching were also observed. Phialides were integrated into the terminal or lateral conidiophores, and were monophialidic, and rarely polyphialidic. Phialides arising directly from the mycelia were mainly monophialidic, often polyphialidic; type I phialides were cylindrical, frequently widened at the bases; type II phialides were predominant, one-septate, elongate-ampulliform and attenuated at the bases to navicular, tapering towards the apices; type III phialides were one-septate, mainly cylindrical, often subulate or navicular. Hyphal coils were observed. Conidia were hyaline and mostly oblong-ellipsoidal to reniform or allantoid, biguttulate, and occasionally ovoid (Figure 3). No perithecium formation was observed under laboratory conditions. The colonies reached a radius of 25-33 mm after 16 d at 23±2 °C. Minimum temperature for growth was 15°C, with optimum of 25 to 30 °C, and maximum of 35°C. The strains belonging to sub-groups #4, #5 and #6 reached a colony radius of 5 mm at 37°C.
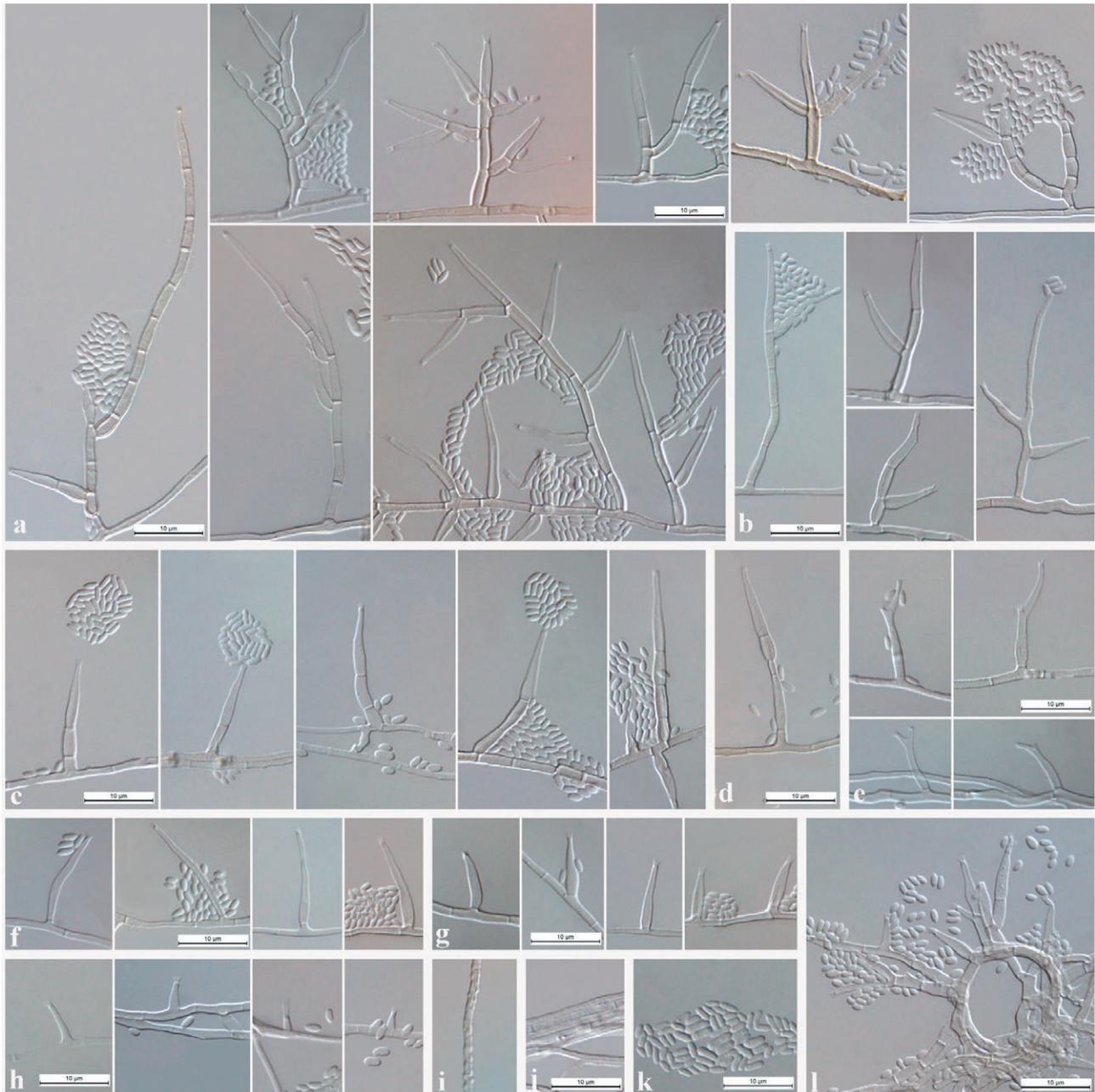
**Figure 3.** Representative light micrographs (Nomarski differential interference contrast) of *Phaeoacremonium italicum*. (**a**) Branched conidiophores; (**b**) unbranched conidiophores with lateral phialides; (**c**) unbranched septate conidiophores; (**d**) conidiophores showing percurrent rejuvenation; (**e**) polyphialides; (**f**) Type III phialides; (**g**) Type II phialides; (**h**) Type I phialides; (**i**) mycelia, showing prominent exudate droplets observed as warts; (**j**) mycelia occurring in bundles; (**k**) conidia; (**l**) hyphal coils.

The morphology and colour of the colonies were variable among the isolates that belonged to the six sub-groups (Table 3; Figure 4). Yellow pigment was observed on OA for strains that belonged to sub-groups #4 and #5 (Figure 4).

Strain CBS 113590, in sub-group #7 had mycelium with branched septate hyphae occurring singly or in bundles; hyphae were tuberculate with sub-hyaline to pale brown, verruculose to smooth warts. Unbranched conidiophores predominated, and were generally one- or two-septate (up to four-) septate and each ending in a single terminal phialide, often bearing one lateral phialide (mainly of type II) next to the terminal phialide; percurrent rejuvenation was rarely observed (Figure 5).
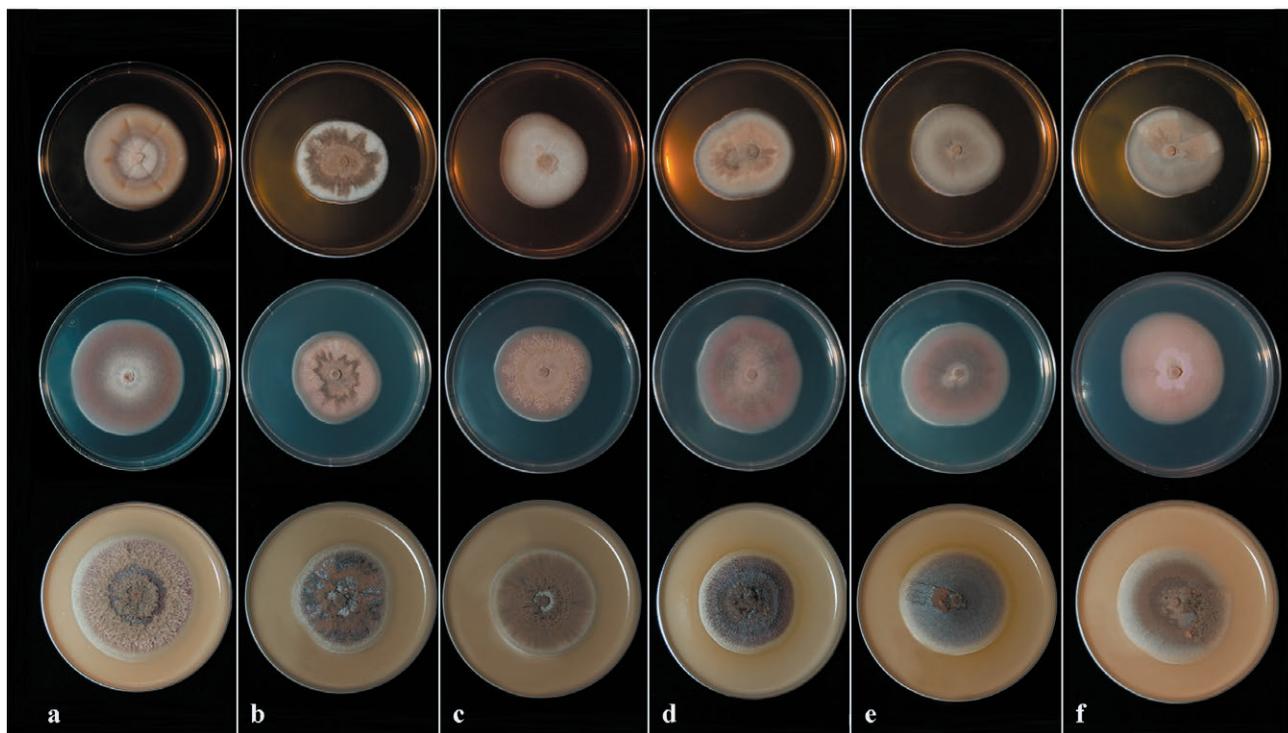
**Figure 4.** Representative culture morphologies for *Phaeoacremonium italicum*. The cultures were grown at 25°C on malt extract agar (top row), potato dextrose agar (middle) and oatmeal agar (bottom row) for 21 d. (**a**) CBS 137763 strain, representing sub-group #1; (**b**) Pm31 strain, subgroup #2; (**c**) Pm50M strain, sub-group #3; (**d**) Pm45 strain, sub-group #4; (**e**) Pm17 strain, sub-group #5; (**f**) Pm59 strain, sub-group #6.

Branched conidiophores were less frequently observed, with few levels of ramification. Phialides were integrated into the conidiophores terminally and laterally, and arose directly from the mycelia. These phialides were mainly monophialidic but occasionally polyphialidic. Type I phialides were cylindrical, occasionally widened at the base. Type II phialides were one-septate, subcylindrical to navicular, tapering towards the apex. Type III phialides predominated, and were one-septate, mainly navicular to subcylindrical, and occasionally subulate. Hyphal coils were observed. Conidia were hyaline and mostly oblong ellipsoidal to obovoid, frequently biguttulate, and occasionally reniform to allantoid (Figure 5). No perithecium formation was observed under laboratory conditions. The colonies reached a radius of 38–43 mm after 16 d at 23±2°C. The minimum temperature for growth was 15°C, with optimum growth at 30°C, and the maximum temperature for growth was of 37°C. Yellow pigment was produced in OA cultures (Figure 5).

*Phylogenetic analyses*

Model Finder Plus was used to detect the best-fit DNA substitution models for the β-tubulin and actin genes and for the IGS datasets. The optimum models were: for the β-tubulin gene, the Kimura 2-parameter with invariable site and discrete gamma distribution (K2P+I+G4) (lnL = -3979.7536), and for the actin gene, the Kimura 2-parameter with invariable sites (K2P+I) (lnL = -1726.3321). The calculated parameters for the β-tubulin gene were: assumed nucleotide frequencies, A = 0.250, G = 0.250, T = 0.250 and C = 0.250; substitution rate matrix with A→C substitution = 1.000, A→G = 3.908, A→T = 1.000, C→G = 1.000, C→T = 3.908, and G→T = 1.000; proportion of invariable sites (I) = 0.342, and gamma distribution (G4) with shape parameter = 1.994. The calculated parameters for the actin gene were: assumed nucleotide frequencies, A = 0.250, G = 0.250, T = 0.250 and C = 0.250; substitution rate matrix with A→C substitution = 1.000, A→G = 4.257, A→T = 1.000, C→G = 1.000, C→T = 4.257 and G→T = 1.000; proportion of invariable sites (I) = 0.442.

The optimum model selected for the IGS fragment was the Transversion model with empirical base frequencies and gamma distribution (TVM+F+G4) (lnL = -22064.046). The calculated parameters were: assumed nucleotide frequencies, A = 0.186, G = 0.288, T = 0.234, and C = 0.292; substitution rate matrix with A→C substi-
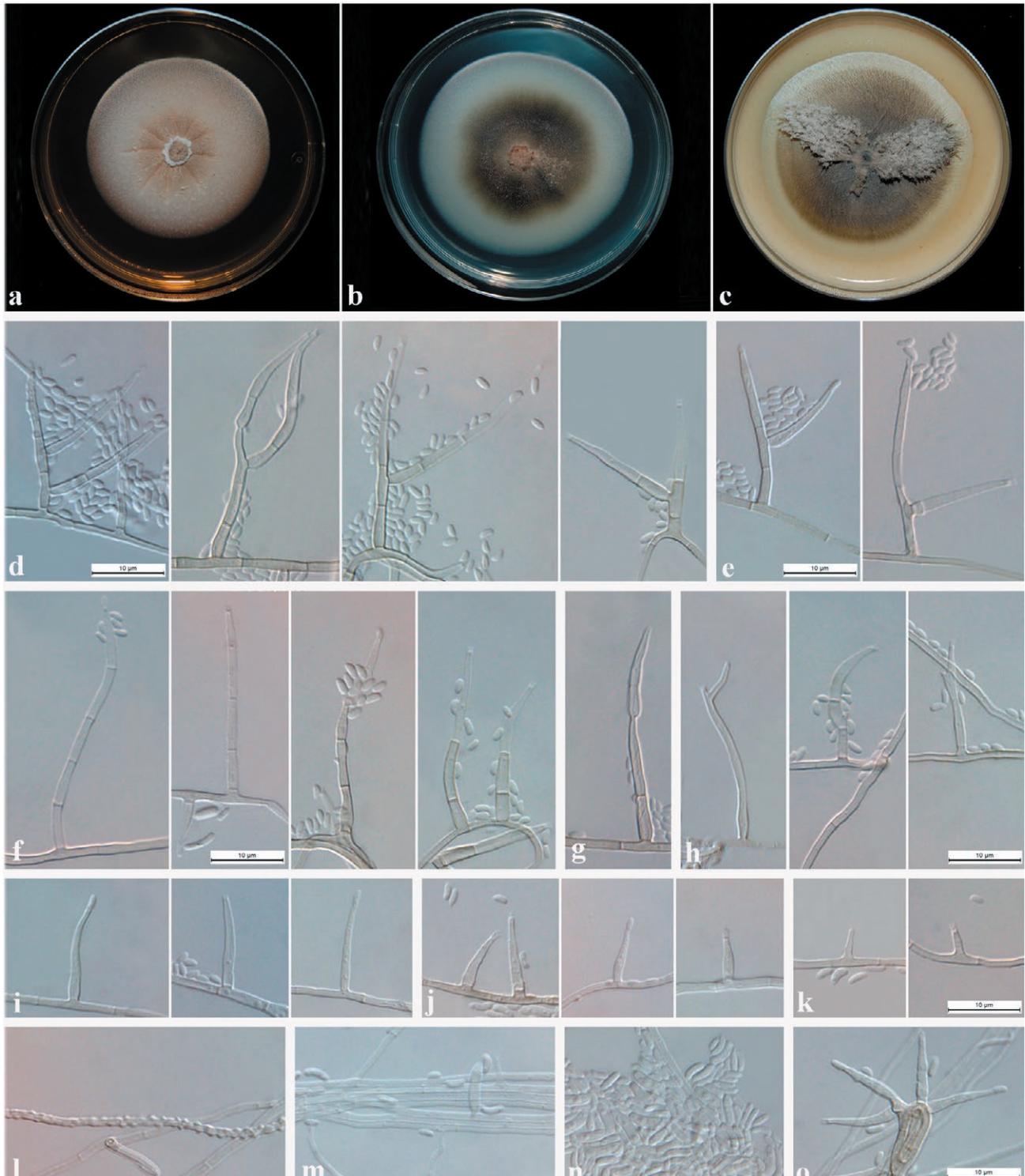
**Figure 5.** Representative light micrographs (Nomarski differential interference contrast) of *Phaeoacremonium alvesii* CBS 113590 as the representative strain of sub-group #7. Twenty-one-day-old colonies grown on malt extract agar (**a**), potato dextrose agar (**b**) and oatmeal agar (**c**) at 23±2°C; (**d**) branched conidiophores; (**e**) unbranched conidiophores with lateral phialides; (**f**) unbranched septate conidiophores; (**g**) conidiophores with percurrent rejuvenation; (**h**) polyphialides; (**i**) Type III phialides; (**j**) Type II phialides; (**k**) Type I phialides; (**l**) hyphae with prominent exudate droplets observed as warts; (**m**) hyphae occurring in bundles; (**n**) conidia; (**o**) hyphal coils.

**Table 3.** Morphological features of *Phaeoacremonium italicum* sub-groups in culture.

| Feature | | Sub-group | | | | | | |
|---|---|---|---|---|---|---|---|---|
| | #1 | #2 | #3 | #4 | #5 | #6 | #7 |
| Representative isolate | CBS 137763 | Pm31 | Pm50M | Pm45 | Pm17 | Pm59 | CBS 113590 |
| Bundles | Yes | Yes | Yes | Yes | Yes | Yes | Yes |
| Warts | Yes | Yes | Not observed | Not observed | Yes | Not observed | Yes |
| **Conidiophores: unbranched (μm)** | | | | | | | |
| Length | (12.3–)19.7–24.8(–47.8) | (11.8–)16.1–21.3(–38.4) | (10.0–)14.9–18.8(–35.4) | (11.1–)14.5–17.8(–28.9) | (8.6–)14.5–21.16(–43.8) | (9.14–)15.05–18.7(–26.6) | (15.1–)21.3–23.9(–43.2) |
| Width | (1.0–)1.5–1.8(–2.4) | (0.38–)1.24–1.43(–1.8) | (1.0–)1.2–1.3(–1.6) | (0.8–)1.2–1.4(–1.7) | (1.0–)1.3–1.5(–1.8) | (0.8–)1.2–1.3(–1.5) | (1.2–)1.6–1.7(–2.2) |
| Mean | 22.3×1.7 | 18.7 × 1.3 | 16.93×1.29 | 16.2×1.3 | 17.8×1.4 | 16.9×1.2 | 22.6×1.7 |
| Number of septa | Up to 7 septate; commonly 2-3 | Up to 7 septate; commonly 3-4 | Up to 6 septate; commonly 3-4 | Up to 5 septate; commonly 3-4 | Up to 9 septate; commonly 4-5 | Up to 5 septate; commonly 3-4 | Up to 3 septate; commonly 2 |
| **Conidiophores: branched (μm)** | | | | | | Less frequent | |
| Length | (21.3–)32.3–40.2(–58.2) | (16.1–)25.9–32.1(–47.3) | (14.6–)25.2–32.3(–48.2) | (17.5–)24.1–30.7(–47.8) | (11.7–)20.5–27.5(–47.8) | (18.7–)32.2–40.7(–65.2) | (18.0–)25.0–31.7(–40.3) |
| Width | (1.2–)1.4–1.5(–1.8) | (1.0–)1.3–1.49(–1.9) | (0.9–)1.2–1.4(–1.6) | (0.84–)1.2–1.4(–2.1) | (0.9–)1.2–1.3(–1.7) | (0.8–)1.2–1.4(–2.1) | (0.9–)1.5–1.8(–2.2) |
| Mean | 36.3×1.5 | 29.0×1.4 | 28.7×1.3 | 25.2×1.3 | 24.0×1.2 | 36.4×1.3 | 28.3×1.7 |
| **Phialide type I (μm)** | | | | | | | |
| Length | (2.1–)5.3–7.3(–11.3) | (1.7–)3.8–4.9(–7.9) | (2.1–)4.1–5.1(–7.2) | (1.1–)2.7–3.7(–5.8) | (1.7–)3.3–4.3(–6.5) | (1.5–)3.7–4.6(–7.6) | (2.9–)4.2–6.7(–11.0) |
| Width | (0.6–)1.2–1.4(–1.8) | (0.5–)0.9–1.1(–1.5) | (0.7–)0.9–1.0(–1.3) | (0.3–)0.8–1.1(–1.7) | (0.7–)0.9–1.1(–1.5) | (0.5–)0.9–1.0(–1.5) | (0.7–)1.0–1.2(–1.7) |
| Mean | 6.3×1.3 | 4.8×1.0 | 4.6×0.9 | 3.2×0.9 | 3.8×1.0 | 4.2×1.0 | 6.5×1.1 |
| Shape | Cylindrical | Cylindrical, sometimes widened at the base | Cylindrical sometimes widened at the base | Cylindrical and slightly widened at the base | Cylindrical | Cylindrical and sometimes widened at the base | Cylindrical, sometimes widened at the base |
| **Phialide type II (μm)** | | | | | | | |
| Length | (5.2–)8.8–10.2(–14.9) | (6.0–)7.9–9.0(–11.1) | (5.9–)7.9–9.1(–13.7) | (5.1–)6.4–7.6(–11.4) | (5.0–)6.4–7.3(–9.4) | (5.3–)7.4–8.5(–10.5) | (9.1–)12.5–13.2(–14.1) |
| Width | (0.9–)1.2–1.4(–1.85) | (0.3–)1.3–1.4(–1.8) | (0.8–)1.2–1.3(–1.6) | (0.2–)1.3–1.6(–2.1) | (0.7–)1.2–1.4(–1.8) | (1.0–)1.3–1.4(–1.7) | (1.1–)1.5–1.6(–2.1) |
| Mean | 9.5×1.4 | 8.5×1.4 | 8.5×1.2 | 7.0×1.4 | 6.9×1.3 | 7.9×1.3 | 12.1×1.5 |
| Shape | Elongate-ampulliform to navicular (predominant) | Elongate-ampulliform to navicular (predominant) | Elongate-ampulliform to navicular (predominant) | Elongate-ampulliform to navicular (predominant) | Navicular to elongate-ampulliform (predominant) | Elongate-ampulliform to navicular (predominant) | Subcylindrical to navicular |
| **Phialide type III (μm)** | | | | | | | |
| Length | (10.7–)12.7–14.2(–20.6) | (10.1–)10.8–12.1(–13.7) | (10.7–)11.6–12.5(–14.1) | (10.1–)10.8–12.4(–14.4) | (10.0–)10.9–12.8(–14.7) | (10.1–)10.9–11.9(–13.4) | (12.0–)14.2–16.1(–19.9) |
| Width | (0.9–)1.3–1.5(–1.8) | (0.9–)1.0–1.2(–1.5) | (0.9–)1.1–1.2(–1.4) | (0.6–)0.9–1.3(–1.6) | (0.7–)1.0–1.3(–1.6) | (1.1–)1.1–1.2(–1.4) | (0.8–)1.5–1.6(–2.4) |
| Mean | 13.5×1.4 | 11.4×1.1 | 12.1×1.6 | 11.6×1.1 | 11.9×1.2 | 11.5×1.2 | 15.9×1.5 |

(Continued)

Table 3. (Continued).

| Feature | Sub-group | | | | | | |
|---|---|---|---|---|---|---|---|
| | #1 | #2 | #3 | #4 | #5 | #6 | #7 |
| Shape | Cylindrical to subulate | Cylindrical to subulate | Subulate to cylindrical | Cylindrical to navicular, rarely subulate | Cylindrical to subulate | Cylindrical to navicular | Navicular to subcylindrical, sometimes subulate (predominant) |
| Polyphialides | Yes | Few | Yes | Few | Yes | Yes | Yes |
| Rejuvenation | Yes | Yes | Yes | Yes | Yes | Yes | Yes |
| Coils | Few | Few | Yes | Yes | Yes | Yes | Few |
| **Conidia (mm)** | | | | | | | |
| Length | (2.1–)2.5–2.7(–3.2) | (1.5–)2.1–2.6(–4.32) | (2.1–)2.5–2.8(–3.5) | (1.3–)2.5–2.9(–4.4) | (1.5–)1.9–2.1(–2.9) | (1.4–)2.4–2.8(–4.4) | (2.4–)3.2–3.5(–4.6) |
| Width | (0.6–)1.0–1.1(–1.4) | (0.6–)0.9–1.1(–1.5) | (0.7–)0.9–0.9(–1.2) | (0.7–)0.94–1.1(–1.6) | (0.6–)0.8–0.8(–1.0) | (0.7–)0.9–0.9(–1.5) | (0.8–)1.1–1.2(–1.9) |
| Mean | 2.6×1.1 | 2.4×1.1 | 2.7×0.9 | 2.7×1.0 | 1.9×0.8 | 2.6×0.9 | 3.4×1.1 |
| Shape | Oblong-ellipsoidal to reniform or allantoid, occasionally ovoid | Oblong-ellipsoidal to allantoid, guttulate | Oblong-ellipsoidal and guttulate, occasionally reniform | Oblong-ellipsoidal to allantoid, guttulate | Oblong-ellipsoidal to allantoid, guttulate | Oblong-ellipsoidal and guttulate, occasionally reniform to allantoid | Obovoid or oblong ellipsoidal, occasionally reniform to allantoid |
| Yellow pigment | No | No | No | Yes | Yes | No | Yes |
| **Colony colour** | | | | | | | |
| On MEA* | Light Greyish Olive (21″b) to Fawn (13″) to Tilleul Buff (17″f) | Vinaceous-Buff (17″d) to White at margin and Army Brown (13″i) to Fawn (13″) at the centre | Cream-Buff (19″d) on the entire colony | Vinaceous Buff (17″d) at margin to Fawn (13″) with irregular sectors Amber Brown (13k) at the centre | Vinaceous-Buff (17″d) to Fawn (13″) in the centre | Vinaceous-Buff (17″d) to Fawn (13″) in the centre with irregular sectors of aerial mycelium Vinaceous-Buff (17″d) to Fawn(13″) | Cameo Brown (7″k) to Vinaceous-Buff (17″d) to Fawn (13″) in the centre |
| On PDA* | Vinaceous-Buff (17″d) to Purplish Vinaceous (1″b) to Tilleul buff (17″f) | Vinaceous-Buff (17″d) at margin with Hazel ring (11′k) to Brownish Vinaceous (5″b) with irregular ring Army Brown(13″i) becoming Fawn (13″) at the centre | Vinaceous-Buff (17″d) at margin to Brownish Vinaceous (5″b) to Fawn (13″) to Light Grayish Vinaceous (9″d) at the centre | Vinaceous Buff (17″d) at margin to Pale Brownish Vinaceous (5″f) becoming Dark Livid Brown (1″k) toward the centre and Pale Vinaceous-Fawn (13″f) at the centre | Vinaceous-Buff (17″d) to Pale Brownish Vinaceous (5″f) becoming Deep Brownish Vinaceous (5″) to Fawn (13″) in the centre | Vinaceous-Buff (17″d) to at margin (19′d) to Onion-skin Pink (11″b) with irregular ring Mauve (63′b) and Yellowish Olive (23″k) to Fawn (13″) | Cream Buff (19′d) to Hazel (11′k) to Isabella colour (19″i) to Hazel (11′k) at the centre |

(Continued)

**Table 3.** (Continued).

| Feature | Sub-group | | | | | | |
|---|---|---|---|---|---|---|---|
| | #1 | #2 | #3 | #4 | #5 | #6 | #7 |
| On OA* | Olive (21"m) to Cream-Buff (19'd) above and reverse with Avellaneous (17"'b) in the centre | Vinaceous-Buff (17"d) to Vinaceous Purple (65"') with aerial mycelium Brownish-Vinaceous (5"'b) at the centre | Vinaceous-Buff (17"d) becoming Army Brown (13"'i) to Bone Brown (13"'m) towards the centre | Vinaceous Buff (17"d) at the margin with Vinaceous Purple (65"') with rare aerial mycelium Brownish-Vinaceous (5"'b) at the centre | Vinaceous Buff (17"d) at the margin with Vinaceous Purple (65"') with rare aerial mycelium Brownish-Vinaceous (5"'b) at the centre | Vinaceous-Buff (17"d) at margin to Army Brown (13"'i) with irregular sectors of aerial mycelium Vinaceous-Buff (17"d) to Army Brown (13"'i) at the centre | Vinaceous-Buff (17"d) at margin to Hazel (11'k) to Sepia (17"'m) with irregular sectors of aerial mycelium Vinaceous-Buff (17"d) |
| **Growth temperatures on MEA\* (°C)** | | | | | | | |
| Minimum | 17 | 15 | 15 | 15 | 15 | 15 | 15 |
| Optimum | 25 | 25 | 30 | 30 | 30 | 25 | 30 |
| Maximum | 35 | 35 | 35 | 35 | 35 | 35 | 37 |
| Radial growth (mm; 16 d, 23±2°C) | 20–25 | 28–32 | 28–33 | 28–32 | 28–33 | 27–33 | 39–43 |

\* MEA, malt extract agar; PDA, potato dextrose agar; OA, oatmeal agar.

tution = 1.014, A→G = 4.371, A→T = 2.087, C→G = 1.273, C→T = 4.371 and G→T = 1.000; rates for variable sites were assumed to follow a gamma distribution (G4) with shape parameter = 0.513.

The partition homogeneity test for the β-tubulin and actin sequences of *Phaeoacremonium* spp. produced a *P*-value of 0.61, which indicated that the dataset was congruent and the two genes could be combined. The combined β-tubulin and actin dataset consisted of 59 taxa, which included the outgroup taxon *P. richardsiae*, and contained 864 characters (β-tubulin, 594; actin, 270; including alignment gaps), of which 416 were constant (β-tubulin, 282; actin, 134), while 27 were variable and parsimony uninformative. Maximum likelihood analysis of the remaining 421 parsimony informative characters (β-tubulin, 296; actin, 125) produced a consensus tree with a Log-likelihood (lnL) = -5742.620763. Maximum parsimony analysis resulted in one most-parsimonious tree (*TL* = 1071; *CI* = 0.675; *RI* = 0.889; *RC* = 0.600; *HI* = 0.325) with similar topology to the maximum likelihood shown in Figure 6 (TreeBASE S28462). The phylogenetic tree obtained by combined analysis of the β-tubulin and actin genes clustered the *Phaeoacremonium* strains into 15 distinct clades, confirming the BLAST identification.

The *P. italicum* strains that belonged to sub-groups #1 to #6 clustered in a single clade that showed intraspecific genetic variation, with bootstrap values ranging from 80 to 98%. Strain CBS 113590 that belonged to sub-group #7 clustered in a sister clade of *P. italicum* (as already reported by Spies *et al.* (2018), with bootstrap support of 80% for maximum parsimony and 98% for maximum likelihood (Figure 6).

The IGS dataset alignment consisted of 59 taxa that included the outgroup taxon *P. richardsiae* and contained 3451 characters (including alignment gaps), of which 1547 were constant, while 202 were variable and parsimony uninformative. Maximum likelihood analysis of the remaining 1702 parsimony informative characters produced a consensus tree with lnL = -20723.212183. Maximum parsimony analysis resulted in 100 most-parsimonious trees (*TL* = 4170; *CI* = 0.720; *RI* = 0.884; *RC* = 0.637; *HI* = 0.280) with similar topology to maximum likelihood, one of which is shown in Figure 7 (TreeBASE S28463). In the comparison of the tree from the phylogenetic analysis of IGS sequences with the phylogenetic tree obtained in the combined analysis of the β-tubulin and actin sequences, the species segregation and tree topology were similar. Although the topology of the trees is not identical, each species was always well separated, and the clusters and segregation of the species were identical to the β-tubulin and actin phylogenetic tree, except for strain CBS 113590 that belonged to
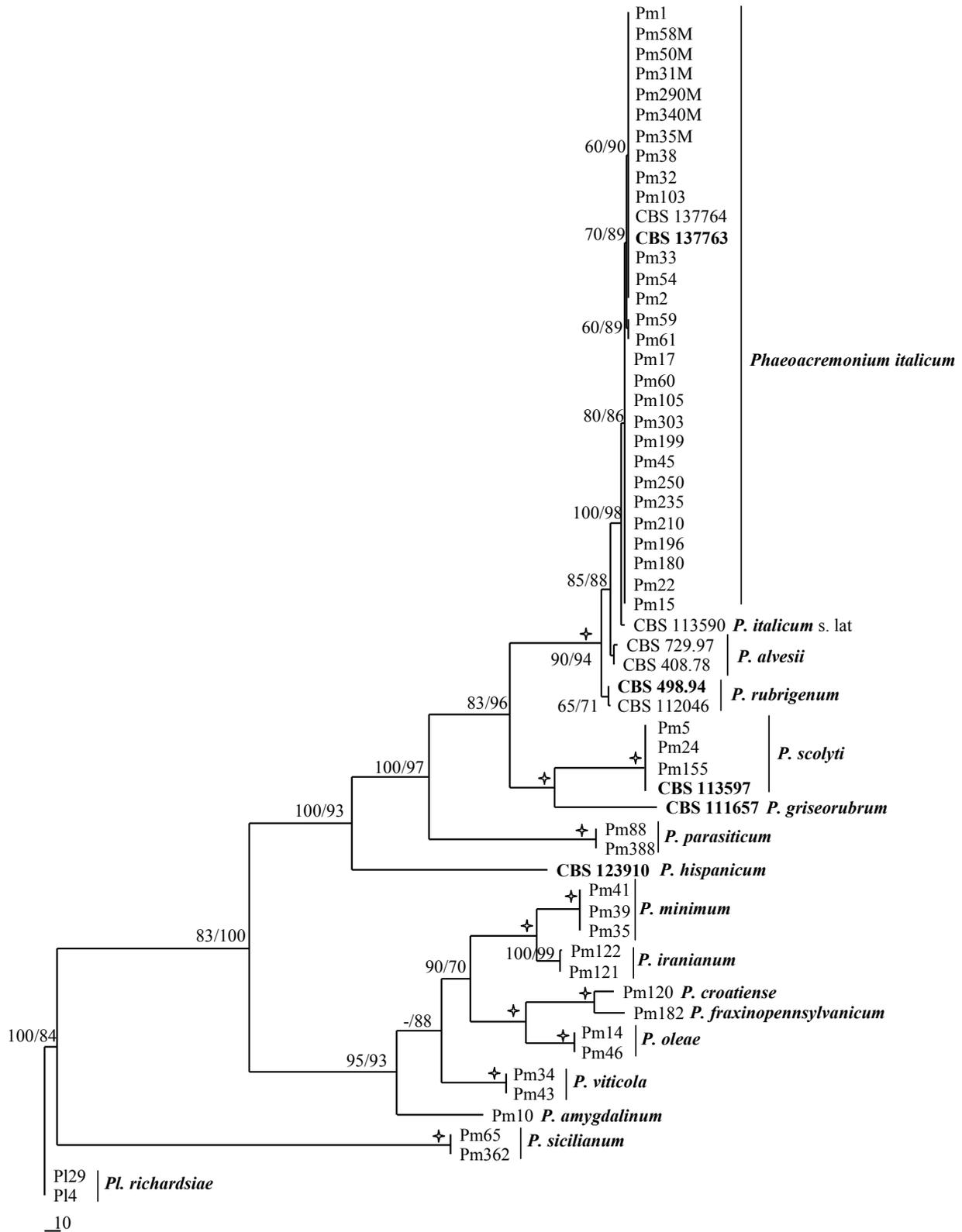
**Figure 6.** The most parsimonious tree obtained from multiple alignment of the β-tubulin and actin genes, with bootstrap values (1000 replicates) from maximum parsimony/maximum likelihood shown at the internodes. Bootstrap values of 100% are indicated with star symbols, and ex-type sequences are highlighted in bold. *Pleurostoma richardsiae* was included as an outgroup.
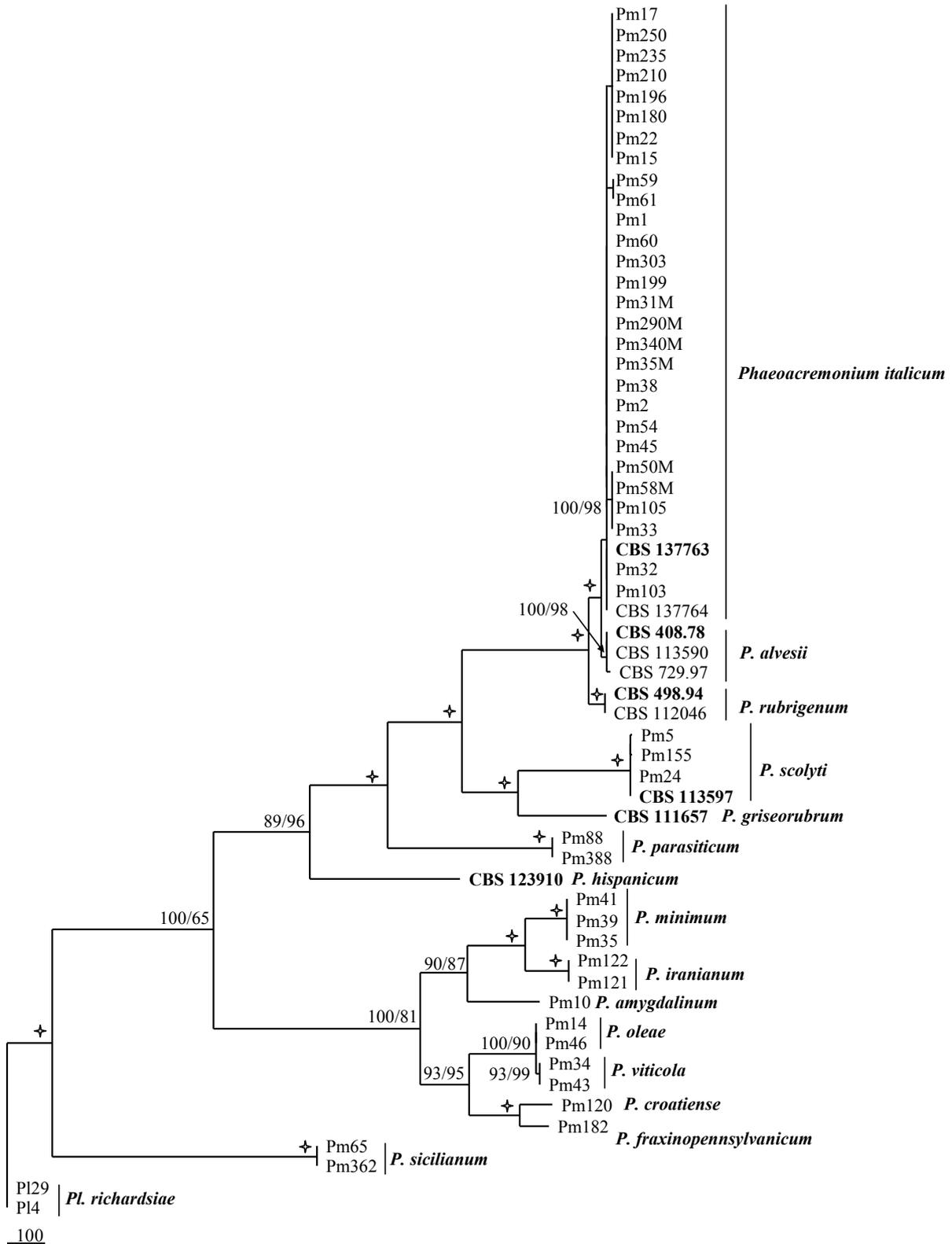
Pm17
Pm250
Pm235
Pm210
Pm196
Pm180
Pm22
Pm15
Pm59
Pm61
Pm1
Pm60
Pm303
Pm199
Pm31M
Pm290M
Pm340M
Pm35M
Pm38
Pm2
Pm54
Pm45
Pm50M
Pm58M
Pm105
Pm33
**CBS 137763**
Pm32
Pm103
CBS 137764
**CBS 408.78**
CBS 113590    *P. alvesii*
CBS 729.97
**CBS 498.94**    *P. rubrigenum*
CBS 112046

*Phaeoacremonium italicum*

100/98

100/98

Pm5
Pm155
Pm24    *P. scolyti*
**CBS 113597**
**CBS 111657**    *P. griseorubrum*
Pm88    *P. parasiticum*
Pm388
**CBS 123910**    *P. hispanicum*

89/96

Pm41    *P. minimum*
Pm39
Pm35
Pm122    *P. iranianum*
Pm121
Pm10    *P. amygdalinum*

90/87

100/65

Pm14    *P. oleae*
Pm46
Pm34    *P. viticola*
Pm43
Pm120    *P. croatiense*
Pm182
*P. fraxinopennsylvanicum*

100/81

100/90

93/95

93/99

Pm65    *P. sicilianum*
Pm362

Pl29    *Pl. richardsiae*
Pl4

100

**Figure 7.** One of the 100 most-parsimonious trees obtained from alignment of the IGS sequences from *Phaeoacremonium* spp., with bootstrap values from 1000 replicates from maximum parsimony/maximum likelihood shown at the internodes. Bootstrap values of 100% are indicated with star symbols, and ex-type sequences are highlighted in bold. *Pleurostoma richardsiae* was included as an outgroup.

*P. italicum* (sub-group #7) (Figures 6 and 7). In the IGS tree, this strain clustered in the clade of *P. alvesii*, with the strains CBS 408.78 and CBS 729.97.

DISCUSSION

In the present analysis of the IGS regions of a population of *P. italicum* strains collected from different hosts and localities, the entire IGS rDNA regions were successfully amplified using standard primers anchored in the conserved 28S and 18S rDNA gene-coding regions. The same standard primers were used to amplify the closest species to *P. italicum*, as *P. alvesii* and *P. rubrigenum*, and also for 12 other *Phaeoacremonium* species.

As the analyses of the complete IGS rDNA sequences of *Phaeoacremonium* spp. revealed the absence of 5S rDNA, in agreement with Drouin and de Sà (1995), we considered that this region was not linked to the rRNA major transcription unit, but was distributed throughout the genomes, as has been reported for several other filamentous fungi (Lockington *et al.,* 1982; Selker *et al.,* 1986; Garber *et al.,* 1988; Walker *et al.,* 2011). Walker *et al.* (2011) attributed the variable gene linkages for 5S in the Eukaryotes to result from stochastic gains and losses of variant repeat units, where functional 5S rRNA had been transposed by the mechanisms that were responsible for the concerted evolution of tandemly repeated multigene families.

Variations were also seen in sequence lengths for the *P. italicum* strains. It is well known that the IGS region is highly variable, as it contains several repeat elements, indels, variable regions with nucleotide substitutions (Albee *et al.,* 1996; James *et al.,* 2001), and sequences called 'repeat motifs' that are essential for initiation of transcription, RNA processing, transcription termination and replication processes of ribosomal DNA (Van't Hof and Lamm, 1991; Fernandez *et al.,* 2000). In the present study, analysis of the distributions of the polymorphisms through the sequences highlighted the presence of five short repeat elements throughout the IGS rDNA region of the *P. italicum* strains, named here as elements A, B, C, P and R. Elements A, B and P and their locations were common to all of the *P. italicum* strains, while the other two elements, C and R showed different number of copies, compositions and distributions among the strains. The presence of these repeated elements and their distributions allowed identification of one polymorphic region (PR) that was flanked by two conserved regions (CR1; CR2). The presence of indels through the IGS sequences was restricted to only the PR. The nucleotide substitutions consisted of insertions and deletions, and transi-

tions and transversions, with these conversely seen only in the CR1 and CR2 regions. A similar organisation was also reported by Pantou *et al.* (2003) for *Metarhizium anisopliae*, Papaioannou *et al.* (2013) for *Verticillium dahliae*, and Durkin *et al.* (2015) for *Colletotrichum lentis*. Papaioannou *et al.* (2013) reported that this organisation putatively reflected the different functions of these sub-regions, and suggested that the highly conserved sub-regions had functions related to rRNA production and processing. The polymorphic sub-region, PR, may be responsible for the promotion of unequal crossing-over events and the maintenance of homogeneity between rDNA complexes (Mirete *et al.,* 2013).

The analysis of these sequences showed that element C was a 'repeat motif', and the intraspecific variation observed among the *P. italicum* strains was mainly due to the number of copies of element C repeated in the IGS rDNA sequences, as well as to the absence of some elements R in the polymorphic region. Diaz *et al.* (2005) reported that repeat motifs in the transcribed region or upstream of the transcription start can act as promoter enhancers and regulators of transcription of rRNA. These could have originated from processes involved in duplication and amplification of short sequences, and from slippage of replication mechanisms. Many such repeat motifs have been described as highly conserved in different Eukaryote species (Diaz *et al.,* 2005). For example, the repeat motif of CAAAAA has been described as a conserved motif in the promoter region of different crucifers, such as *Brassica* spp. (Bhatia *et al.,* 1996), *Raphanus* spp. (Delcasso *et al.,* 1988) and *Arabidopsis* (Gruendler *et al.,* 1991). Other common repeat motifs, such as the TATA motif, are probably involved in assembly of the pre-initiation complex and selection of transcription sites (Melanè *et al.,* 1998). These have been reported as common elements in fungi, including *Schizophyllum commune* (James *et al.,* 2001), *Laccaria bicolor* (Martin *et al.,* 1999) and *Neurospora* spp. (Selker *et al.,* 1986). The high degree of sequence similarities seen for CR1 and CR2 among the *P. italicum* strains can be used in conjunction with the characteristic repeat motifs of the fungus, for the design of species or group-specific primers for intraspecific group detection (Diaz *et al.*, 2005; Papaioannou *et al.,* 2013).

Based on the presence of repeated elements, on the number of copies of some of these elements, and on their composition, the *P. italicum* strains were grouped into seven different sub-groups (#1 to #7). Comparisons of the results of the polymorphic region PR sequences of all of the *P. italicum* strains analysed in this study showed that these were structurally similar across all

of the sub-groups, although some differences were seen among the different *P. italicum* sub-groups. In particular, sub-groups #1 to #6 all shared the same initial layout of R elements in the first part of the polymorphic regions (PR-a), while they varied mainly in the numbers of copies of element C and for the absence of elements R5, R8 and R12 in the second part of polymorphic region (PR-b). Sub-group #7 contained strain CBS 113590, identified as *P. alvesii* by White *et al.* (2011) and Moyo *et al.* (2014), and more recently classified as *P. italicum sensu lato* by Spies *et al.* (2018); here it showed differences in the disposition and composition of the repeated elements.

Comparing the IGS structures of the sub-groups of *P. italicum* with the closest species of *P. alvesii* and *P. rubrigenum*, it was possible to confirm the same kinds of repeated elements, although they were differently organised and sometimes modified. The IGS structure of *P. alvesii* strain CBS 408.78 was identical to that of strain CBS 113590 of sub-group #7. Micromorphological analyses of the representative isolates of each of the *P. italicum* sub-groups showed similarities among sub-groups #1 to #6, and differences for sub-group #7. In comparison with the strains of sub-groups #1 to #6, CBS 113590 had longer and less septate unbranched conidiophores, rarely branched conidiophores, phialides predominantly of type III, ovoid conidia, more rapid growth rate, and maximum cardinal temperature for growth of 37°C. These features resemble those described by Moster *et al.* (2006) for *P. alvesii*. Based on the observations carried out on the strains of *P. italicum* sub-groups #1 to #6, the present study provides an upgrade of the morphological descriptions reported by Raimondo *et al.* (2014). For instance, compared to the original descriptions: the temperature minimum for growth (15°C) and growth optimum (25-30°C) were slightly different; and the morphological traits, such as branched conidiophores, were frequently, rather than occasionally, encountered. The frequent presence of polyphialides was another trait encountered. Based on the detailed examination carried out on this collection of *P. italicum* and *P. alvesii* strains in the present study, yellow pigment production was not to be a reliable feature for distinguishing these two species according to Spies *et al.* (2018). The strains that belonged to *P. italicum* subgroups #4 and #5, as well as CBS 113590 of sub-group #7 and *P. alvesii* (CBS 408.78, CBS 729.97), produced yellow pigment on OA. Therefore, the presence of abundant branched conidiophores, the high numbers of septa of the unbranched conidiophores, the predominance of type II phialides, the smaller sizes of type II and III phialides, the colour of the cultures on different media, and the minimum and maximum cardinal temperatures for growth,

differentiate *P. italicum* from *P. alvesii*. Comparisons of the phylogenetic trees obtained for the combined analysis of β-tubulin and actin sequences with the phylogenetic analysis of the IGS sequences showed identical clustering and segregation of the *Phaeoacremonium* spp., except for strain CBS 113590. The combined analysis of the β-tubulin and actin sequences segregated this strain into a sister clade of *P. italicum,* while the IGS phylogenetic tree clustered it with *P. alvesii.*

The IGS rDNA region has been successfully used to study relationships in other fungi at intraspecific levels, including for *Fusarium oxysporum* (Appel and Gordon, 1996), *Metarhizium anisopliae* (Pipe *et al.,* 1995), *Microdochium nivale* (Mahuku *et al.,* 1998), *Hebeloma cylindrosporium* (Guidot *et al.,* 1999), *Cryptococcus neoformans* (Diaz *et al.,* 2005), *Phomopsis helianthi* (Pecchia *et al.,* 2004), and *Verticillium albo-atrum* (Mahuku and Platt, 2002). The IGS region is one of the most rapidly evolving regions and provides large datasets that are considered to be phylogenetically useful, and these have provided large numbers of informative characters to delineate the relationships within and between species (Hillis and Dixon, 1991).

Based on micromorphological and molecular data, we conclude that the strain CBS 113590 belongs to *P. alvesii* and not to *P. italicum sensu lato*. Further molecular studies on phylogenetic signals and presence of barcoding gap, and multilocus analyses (β-tubulin, actin, and IGS sequences) using a large number of *Phaeoacremonium* strains will be carried out to determine whether the IGS rDNA region is a suitable marker for phylogenetic resolution of *Phaeoacremonium* species, to be used alone or in combination with β-tubulin and actin markers, to avoid misidentifications and introduction of vague species boundaries.

## LITERATURE CITED

Albee S.R., Mueller G.M., Kropp B.R., 1996. Polymorphisms in the large intergenic spacer of the nuclear ribosomal repeat identify *Laccaria proxima* strains. *Mycologia* 88: 970–976.

Appel D.J., Gordon T.R., 1996. Relationships among pathogenic and nonpathogenic isolates of *Fusarium*

*oxysporum* based on the partial sequence of the intergenic spacer region of the ribosomal DNA. *Molecular Plant-Microbe Interactions* 9: 125–138.

Ariyawansa H.A., Hyde K.D., Jayasiri S.C., … Chen X.H., 2015. Fungal diversity notes 111–252: taxonomic and phylogenetic contributions to fungal taxa. *Fungal Diversity* 75: 27–274.

Bhatia S., Negi M.S., Lakshmikumaran M., 1996. Structural analysis of the rDNA intergenic spacer of *Brassica nigra*: evolutionary divergence of the spacers of the three diploid *Brassica* species. *Journal of Molecular Evolution* 43: 460–468.

Calabon M.S., Jones E.B.G., Boonmee S., Doilom M., Lumyong S., Hyde K.D., 2021. Five novel freshwater ascomycetes indicate high undiscovered diversity in lotic habitats in Thailand. *Journal of Fungi* 7: 117–143.

Carlucci A., Lops F., Cibelli F., Raimondo M.L., 2015. *Phaeoacremonium* species associated with olive wilt and decline in southern Italy. *European Journal of Plant Pathology* 141: 717–729.

Carlucci A., Raimondo M.L., Cibelli F., Phillips A.J.L., Lops F., 2013. *Pleurostomophora richardsiae, Neofusicoccum parvum* and *Phaeoacremonium aleophilum* associated with a decline of olives in southern Italy. *Phytopathologia Mediterranea* 52: 517–527.

Crous P.W., Gams W., 2000. *Phaeomoniella chlamydospora* gen. et comb. nov., a causal organism of Petri grapevine decline and esca. *Phytopathologia Mediterranea* 39: 112–118.

Crous P.W., Gams W., Wingfield M.J., Van Wyk P.S., 1996. *Phaeoacremonium* gen. nov. associated with wilt and decline diseases of woody hosts and human infections. *Mycologia* 88: 786–796.

Crous P.W., Wingfield M.J., Burgess T.I., … Groenewald J.Z., 2016. Fungal planet description sheets: 469–557. *Persoonia* 37: 340–341.

Cunningham C.W., 1997. Can three incongruence tests predict when data should be combined? *Molecular Biology Evolution* 14: 733–740.

Da Silva M.A., Correia K.C., Barbosa M.A.G., Camara M.P.S., Gramaje D., Michereff S.J., 2017. Characterization of *Phaeoacremonium* isolates associated with Petri disease of table grapes in northeastern Brazil, with description of *Phaeoacremonium nordesticola* sp. nov. *European Journal of Plant Pathology* 149: 695–709.

Damm U., Mostert L., Crous P.W., Fourie P.H., 2008. Novel *Phaeoacremonium* species associated with necrotic wood of *Prunus* trees. *Persoonia* 20: 87–102.

Delcasso-Tremousaygue D., Grellet F., Panabieres F., Ananiev E.D., Delseney M., 1988. Structural and transcriptional characterization of the external spacer of a ribosomal RNA nuclear gene from a higher plant. *European Journal of Biochemistry* 172: 767–776.

Diaz M.R., Boekhout T., Kiesling T., Fell J.W., 2005. Comparative analysis of the intergenic spacer regions and population structure of the species complex of the pathogenic yeast *Cryptococcus neoformans*. *FEMS Yeast Research* 5: 1129–1140.

Dissanayake M.L.M.C., Kashima R., Tanaka S., Ito S.I., 2009. Genetic diversity and pathogenicity of *Fusarium oxysporum* isolated from wilted Welsh onion in Japan. *Journal of General Plant Pathology* 75: 125–130.

Drouin G., de Sà M.M., 1995. The concerted evolution of 5S ribosomal genes linked to the repeat units of other multigene families. *Molecular Biology and Evolution* 12: 481–493.

Durkin J., Bissett J., Pahlavani M., Mooney B., Buchwaldt L., 2015. IGS minisatellites useful for race differentiation in *Colletotrichum lentis* and a likely site of small RNA synthesis affecting pathogenicity. *PLoS One* 10: e0137398.

Essakhi S., Mugnai L., Crous P.W., Groenewald J.Z., Surico G., 2008. Molecular and phenotypic characterisation of novel *Phaeoacremonium* species isolated from esca diseased grapevines. *Persoonia* 21: 119–134.

Fernandez M., Polanco C., Ruiz M.L., Perez de la Vega M., 2000. A comparative study of the structure of the rDNA intergenic spacer of *Lens culinaris* Medik. and other legume species. *Genome* 43: 597–602.

Garber R.C., Turgeon B.G., Selker E.U., Yoder O.C., 1988. Organization of ribosomal RNA genes in the fungus *Cochliobolus heterostrophus*. *Current Genetics* 14: 573–582.

Gramaje D., Mostert L., Groenewald J.Z., Crous P.W., 2015. *Phaeoacremonium*: from esca disease to phaeohyphomycosis. *Fungal Biology* 119: 759–783.

Gruendler P., Unfried I., Pointne R., Schweizer C., 1991. Nucleotide sequence of the 25S-18S ribosomal gene spacer from *Arabidopsis thaliana*. *Nucleic Acids Research* 17: 6395–6396.

Guidot A., Lumini E., Debaud J.C., Marmeisse R., 1999. The nuclear ribosomal DNA intergenic spacer as a target sequence to study intraspecific diversity of the ectomycorrhizal basidiomycete *Hebeloma cylindrosporum* directly on *Pinus* root systems. *Applied Environmental Microbiology* 65: 903–909.

Hawksworth D.L., Crous P.W., Redhead S.A., Scott A., Reynolds Don R., … Frisvad J.C., 2011. Fungal nomenclature 2. The Amsterdam declaration on fungal nomenclature. *Mycotaxon* 116: 491–500.

Hillis D.M., Dixon M.T., 1991. Ribosomal DNA: molecular evolution and phylogenetic inference. *The Quarterly Review of Biology* 66: 411–453.

Hoang D.T., Chernomor O., von Haeseler A., Minh B.Q., Vinh L.S., 2018. UFBoot2: Improving the Ultrafast Bootstrap Approximation. *Molecular Biology Evolution* 5: 518–522.

James T.Y., Moncalvo J.M., Li S., Vilgalys R., 2001. Polymorphism at the ribosomal DNA spacers and its relation to breeding structure of the widespread mushroom *Schizophyllum commune*. *Genetics* 157: 149–161.

Jayawardena R.S., Purahong W., Zhang W., Wubet T., Li X.H., Yan J., 2018. Biodiversity of fungi on *Vitis vinifera* L. revealed by traditional and high-resolution culture-independent approaches. *Fungal Diversity* 90: 1–84.

Kalyaanamoorthy S., Minh B.Q., Wong T.K.F., von Haeseler A., Jermiin L.S., 2017. ModelFinder: fast model selection for accurate phylogenetic estimates. *Nature Methods* 14: 587–589.

Katoh F., Frith M.C., 2012.  Adding unaligned sequences into an existing alignment using MAFFT and LAST. *Bioinformatics* 28: 3144–3146.

Katoh K., Standley D.M., 2013. MAFFT multiple sequence alignment software version 7: Improvements in performance and usability. *Molecular Biology Evolution* 30: 772–780.

Lockington R.A., Taylor G.C., Winther M., Scazzocchio C., Davies R.W., 1982. A physical map of the ribosomal DNA repeat unit of *Aspergillus nidulans*. *Gene* 20: 135–137.

Mahuku G.S., Hsiang T., Yang L., 1998. Genetic diversity of *Microdochium nivale* isolates from turfgrass. *Mycological Research* 102: 559–567.

Mahuku G.S., Platt HW., 2002. Molecular evidence that *Verticillium albo-atrum* Grp 2 isolates are distinct from *V. albo-atrum* Grp 1 and *V. tricorpus*. *Molecular Plant Pathology* 3: 71–79.

Martin F., Selosse M.A., Le Tacon F., 1999. The nuclear rDNA intergenic spacer of the ectomycorrhizal basidiomycete *Laccaria bicolor*: structural analysis and allelic polymorphism. *Microbiology* 145: 1605–1611.

Melané A., Vivier M.A., Pretorius I.S., 1998. Identification of a functional TATA element in the STA2 glucoamylase gene promoter from *Saccharomyces cerevisiae*. *Current Genetics* 33: 10–15.

Minh B.Q., Nguyen M.A.T., von Haeseler A., 2013. Ultrafast approximation for phylogenetic bootstrap. *Molecular Biology and Evolution* 30: 1188–1195.

Mirete S., Patiño B., Jurado M., Vázquez C., González-Jaén M.T., 2013. Structural variation and dynamics of the nuclear ribosomal intergenic spacer region in key members of the *Gibberella fujikuroi* species complex. *Genome* 56: 205–213.

Mostert L., Groenewald J.Z., Summerbell R.C., Gams W., Crous P.W., 2006. Taxonomy and pathology of *Togninia* (Diaporthales) and its *Phaeoacremonium* anamorphs. *Studies in Mycology* 54: 1–113.

Mostert L., Groenewald J.Z., Summerbell R.C., Robert V., Sutton D.A., Padhye A.A., Crous P.W., 2005. Species of *Phaeoacremonium* associated with infections in humans and environmental reservoirs in infected woody plants. *Journal of Clinical Microbiology* 43: 1752–1767.

Moyo P., Allsopp E., Roets F., Mostert L., Halleen F., 2014. Arthropods vector grapevine trunk disease pathogens. *Phytopathology* 104: 1063–1069.

Nguyen L.T., Schmidt H.A., von Haeseler A., Minh B.Q., 2015. IQ-TREE: A fast and effective stochastic algorithm for estimating maximum likelihood phylogenies. *Molecular Biology and Evolution* 32: 268–274.

Nigro F., Boscia D., Antelmi I., Ippolito A., 2013. Fungal species associated with a severe decline of olive in southern Italy. *Journal of Plant Pathology* 95: 668.

Olmo D., Armengol J., León M., Gramaje  D., 2015. Pathogenicity testing of lesser-known fungal trunk pathogens associated with wood decay of almond trees. *European Journal of Plant Pathology* 143: 607–611.

Page R.D., 1996. TreeView: an application to display phylogenetic trees on personal computers. *Computer Application in Bioscience* 12: 357–358.

Pantou M.P., Mavridou A., Typas M.A., 2003. IGS sequence variation, group-I introns and the complete nuclear ribosomal DNA of the entomopathogenic fungus *Metarhizium*: excellent tools for isolate detection and phylogenetic analysis. *Fungal Genetics and Biology* 38: 159–174.

Papaioannou I.A., Dimopoulou C.D., Typas M.A., 2013. Structural and phylogenetic analysis of the rDNA intergenic spacer region of *Verticillium dahliae*. *FEMS Microbiological Letters* 347: 23–32.

Pecchia S., Mercatelli E., Vannacci G., 2004. Intraspecific diversity within *Diaporthe helianthi*: evidence from rDNA intergenic spacer (IGS) sequence analysis. *Mycopathologia* 157: 317–326.

Pipe N.D., Chandler D., Bainbridge B.W., Heale J.B., 1995. Restriction length polymorphisms in the ribosomal RNA gene complex of isolates of the entomopathogenic fungus *Metarhizium anisopliae*. *Mycological Research* 99: 485–491.

Raimondo M.L., Lops F., Carlucci A., 2014. *Phaeoacremonium italicum* sp. nov., associated with esca of grapevine in southern Italy. *Mycologia* 106: 1119–1126.

Rayner R.W., 1970. *A mycological colour chart*. Commonwealth Mycological Institute, Kew, Surrey, UK.

Sampietro D.A., Marín P., Iglesias J., Presello D.A., Vattuone M.A., …González-Jaén M.T., 2010. A molecular based strategy for rapid diagnosis of toxigenic *Fusarium* species associated to cereal grains from Argentina. *Fungal Biology* 114: 74–81.

Selker E.U., Morzycka-Wroblewska E., Stevens J.N., Metzenberg R.L., 1986. An upstream signal is required for *in-vitro* transcription of *Neurospora* 5S RNA genes. *Molecular Genetics and Genomics* 205: 189–192.

Sohrabi M., Mohammadi H., Leon M., Armengol J., Banihashemi Z., 2020. Fungal pathogens associated with branch and trunk cankers of nut crops in Iran. *European Journal of Plant Pathology* 157: 327–351.

Soltaninejad N., Mohammadi H., Massumi H., 2017. Isolation, identification and pathogenicity of Botryosphaeriaceae and *Phaeoacremonium* species associated with decline of *Prunus* species in Iran. *Journal of Plant Pathology* 99: 571–581.

Spies C.F.J., Moyo P., Halleen F., Mostert L., 2018. *Phaeoacremonium* species diversity on woody hosts in the Western Cape Province of South Africa. *Persoonia* 40: 26–62.

Sugita T., Nakajima M., Ikeda R., Matsushima T., Takako S., 2002. Sequence analysis of the ribosomal DNA intergenic spacer 1 regions of *Trichosporon* species. *Journal of Clinical Microbiology* 40: 1826–1830.

Swofford D.L., PAUP*. 2003. *Phylogenetic Analysis Using Parsimony, Version 4.* Sinauer Associates, Sunderland, UK.

Úrbez-Torres J.R., Haag P., Bowen P., O'Gorman D.T., 2014. Grapevine trunk diseases in British Columbia: incidence and characterization of the fungal pathogens associated with Esca and Petri disease of grapevine. *Plant Disease* 98: 469–482.

Van't Hof J., Lamm S.S., 1991. Single stranded replication intermediates of ribosomal DNA replicons of pea. *The EMBO Journal* 10: 1949–1953.

Walker A.S., Bouguennec A., Confais J., Morgant G., Leroux P., 2011. Evidence of host-range expansion from new powdery mildew (*Blumeria graminis*) infections of triticale (× Triticosecale) in France. *Plant Pathology* 60: 207–220.

White C.L., Halleen F., Fischer M., Mostert L., 2011. Characterisation of the fungi associated with esca diseased grapevines in South Africa. *Phytopathologia Mediterranea* 50: 204–223.